Received: 12 May 2022 | Revised: 14 February 2023 | Accepted: 3 April 2023

DOI: 10.1002/eap.2858

ARTICLE

ECOLOGICAL APPLICATIONS
ECOLOGICAL SOCIETY OF AMERICA

Modeling impacts of saltwater intrusion on methane and nitrous oxide emissions in tidal forested wetlands

Hongqing Wang[1] | **Zhaohua Dai**[2,3] | **Ken W. Krauss**[4] | **Carl C. Trettin**[2] | **Gregory B. Noe**[5] | **Andrew J. Burton**[3] | **Eric J. Ward**[4]

[1]U.S. Geological Survey, Wetland and Aquatic Research Center, Baton Rouge, Louisiana, USA

[2]USDA Forest Service, Center for Forested Wetlands Research, Cordesville, South Carolina, USA

[3]Michigan Technological University, College of Forest Resources and Environmental Science, Houghton, Michigan, USA

[4]U.S. Geological Survey, Wetland and Aquatic Research Center, Lafayette, Lafayette, Louisiana, USA

[5]U.S. Geological Survey, Florence Bascom Geoscience Center, Reston, Virginia, USA

Correspondence
Hongqing Wang
Email: wangh@usgs.gov

Funding information
Forest Service; NASA; U.S. Geological Survey (USGS)

Handling Editor: Hinsby Cadillo-Quiroz

Abstract

Emissions of methane (CH_4) and nitrous oxide (N_2O) from soils to the atmosphere can offset the benefits of carbon sequestration for climate change mitigation. While past study has suggested that both CH_4 and N_2O emissions from tidal freshwater forested wetlands (TFFW) are generally low, the impacts of coastal droughts and drought-induced saltwater intrusion on CH_4 and N_2O emissions remain unclear. In this study, a process-driven biogeochemistry model, Tidal Freshwater Wetland DeNitrification-DeComposition (TFW-DNDC), was applied to examine the responses of CH_4 and N_2O emissions to episodic drought-induced saltwater intrusion in TFFW along the Waccamaw River and Savannah River, USA. These sites encompass landscape gradients of both surface and porewater salinity as influenced by Atlantic Ocean tides superimposed on periodic droughts. Surprisingly, CH_4 and N_2O emission responsiveness to coastal droughts and drought-induced saltwater intrusion varied greatly between river systems and among local geomorphologic settings. This reflected the complexity of wetland CH_4 and N_2O emissions and suggests that simple linkages to salinity may not always be relevant, as non-linear relationships dominated our simulations. Along the Savannah River, N_2O emissions in the moderate-oligohaline tidal forest site tended to increase dramatically under the drought condition, while CH_4 emission decreased. For the Waccamaw River, emissions of both CH_4 and N_2O in the moderate-oligohaline tidal forest site tended to decrease under the drought condition, but the capacity of the moderate-oligohaline tidal forest to serve as a carbon sink was substantially reduced due to significant declines in net primary productivity and soil organic carbon sequestration rates as salinity killed the dominant freshwater vegetation. These changes in fluxes of CH_4 and N_2O reflect crucial synergistic effects of soil salinity and water level on C and N dynamics in TFFW due to drought-induced seawater intrusion.

KEYWORDS

blue carbon, climate change, DeNitrification-DeComposition (DNDC), oligohaline marshes, soil-borne greenhouse fluxes, soil salinity, soil water level, tidal forests

INTRODUCTION

Wetlands store approximately 16%–33% of global soil carbon with only 3% of the terrestrial land surface (Bridgham et al., 2006). Tidal freshwater forested wetlands (TFFW) were recently found to play an important role in sequestering and storing "blue carbon", similar to mangroves, saltmarshes, and seagrass (Krauss et al., 2018). Nevertheless, mineralization of organic carbon to carbon dioxide (CO_2) under both aerobic and anaerobic conditions, and to methane (CH_4) in the absence of oxygen represents an important conduit for carbon loss from TFFW (Krauss & Whitbeck, 2012). Nitrous oxide (N_2O) emissions from nitrogen (N)-loaded salt marshes were found to reduce the blue carbon value of coastal marshes in terms of climate change mitigation potential (Neubauer & Megonigal, 2015; Roughan et al., 2018), with CO_2 and CH_4 emissions together offsetting as much as 94% of the sequestered carbon based on CO_2-equivalents calculations (radiative balance, sensu Neubauer et al., 2022) of greenhouse gas (GHG) emissions (Roughan et al., 2018). Furthermore, the location and low-lying position of TFFW make them vulnerable to environmental change, particularly related to sea-level rise (SLR) (Craft, 2012). TFFW are sensitive to coastal droughts through declines in direct precipitation, lower riverine freshwater discharge, and human alteration of incoming tidal level that affects tidal range and salinity along many rivers (Conrads & Darby, 2017). TFFW are especially vulnerable to saltwater intrusion from SLR, coastal droughts, and heightened frequency and extent of storm surge (Neubauer et al., 2013; Noe et al., 2021; Pierfelice et al., 2015; Thomas et al., 2015).

Soil water level and porewater salinity are critical factors that affect CH_4 and N_2O emissions in TFFW through their interactions on plant growth, mortality, soil and plant respiration, soil organic matter decomposition, methanogenesis, methanotrophy, N/P mineralization, nitrification, denitrification, and other processes (Dai et al., 2018a; Krauss et al., 2012; Liu et al., 2017; Megonigal & Schlesinger, 2002; Noe et al., 2013; Wang et al., 2017; Wang, Dai, Trettin, et al., 2022). With saltwater intrusion, microbial pathways of anaerobic organic matter mineralization shift from methanogenesis to iron reduction and sulfate reduction (Weston et al., 2006), which could reduce relative CH_4 flux with progressive salinization (Holm et al., 2016; Poffenbarger et al., 2011). In trade-off, CH_4 emissions from coastal wetlands were found to be higher at higher water levels, but at low water levels the effect of salinity was more prominent, with highest CH_4 emissions occurring at five practical salinity units (psu) (Liu et al., 2019). Krauss and Whitbeck (2012) found that average salinity at a field site location had no overall effect on CH_4 and N_2O emissions in forested wetlands along the Savannah River, USA, but specific sampling periods did indicate some potential for CH_4 and N_2O flux differentiation seasonally, perhaps related to unaccounted episodic drivers such as soil water level, redox potential, temperature, and soil organic matter content.

Inconsistent and sometimes even opposite responses of CH_4 and N_2O fluxes from the existing, though limited, TFFW studies prevent confirmatory inference and predictive capabilities reflected by real complexity, non-linearity, and spatial and temporal variations of biogeochemical processes and mechanisms in determining GHG emissions (e.g., Anderson & Lockaby, 2007). Both flooding and increasing salinity decreased N_2O emissions in microcosm experiments using TFFW soils; reductions were likely from anaerobic and salinity-induced suppression of nitrification and denitrification (Liu et al., 2017). N_2O production from tidal forest soil incubations collected along three rivers of southeastern Georgia, USA, responded differently with increase in salinity treatments (0, 2, 5 psu): N_2O increased with salinity in Satilla River forest soil incubations due to the inhibition of nitrous oxide reductase at lower pH, but N_2O exhibited no discernable response to salinity from soil incubations along the Altamaha and Ogeechee rivers due to the complete reduction of N_2O to N_2 gas (Marton et al., 2012). Additionally, there are very few studies that examine the synergistic impacts with soil water level fluctuation, specifically the combined effects of drought-induced water depth reductions and soil salinity increases on CH_4 and N_2O emissions in TFFW. Using paired laboratory and field experiments for freshwater forested wetland soils, Helton et al. (2019) found that the magnitude and direction of GHG responses to flooding and marine salt addition depended on the hydrologic context in which marine salt exposure occurred.

Coastal droughts control saltwater intrusion events into the tidal forests along upper river tidal reaches, with salt accumulating in the soil under increased evapotranspiration (Wang et al., 2020a). Therefore, it is predicted that the responses of CH_4 and N_2O emissions in TFFW soils to coastal droughts and drought-induced saltwater intrusion could be even more important to understand than salinity presses from rising sea level, although SLR would dictate where drought-induced saltwater intrusion might occur along any coastal landscape river gradient over longer time periods. The cost of field deployment and maintenance for equipment, such as eddy covariance towers or gas chambers, over a relatively long period hinders the collection of data and information that is required to assess the impact of changing physical conditions on full CH_4 and N_2O emissions budgets for TFFW and transitional oligohaline habitat. Therefore, a process-driven modeling approach is necessary to predict CH_4 and N_2O emissions, as long as synergistic interactions among climate, hydrology, soil, and vegetation are included in relevant ways (e.g., Bridgham et al., 2013). Understanding the production and consumption of carbon under natural and anthropogenic disturbances is part of that need.

A process-driven TFFW biogeochemistry model, called Tidal Freshwater Wetlands (TFW) DeNitrification-DeComposition (DNDC) model, or TFW-DNDC, was developed (Wang, Dai, Trettin, et al., 2022) based on the mangrove version of the DNDC model (Mangrove Carbon Assessment Tool [MCAT], Dai et al., 2018a, 2018b) with necessary modifications to meet the structural and functional requirements of TFFW. MCAT-DNDC integrates biogeochemical processes of Forest-DNDC (Li et al., 2000) and wetland-DNDC (Li et al., 2004; Zhang et al., 2002), which accommodated freshwater wetland biogeochemistry, with new provisions for carbon, nitrogen, and phosphorus processing to incorporate changes in biogeochemical reactions mediated by nutrients, water level, salinity stress, and disturbance regimes (Dai et al., 2018a). TFW-DNDC was applied to examine the responses of plant productivity, plant growth and maintenance respiration, soil respiration, soil organic carbon (SOC) sequestration and storage to drought-induced salinity intrusion in TFFW along the Waccamaw and Savannah rivers in the southeastern United States (Wang, Dai, Trettin, et al., 2022). Biogeochemical processes such as methanogenesis, methanotrophy, soil organic matter decomposition, N/P mineralization, nitrification, and denitrification that affect CH_4 and N_2O emissions are included in TFW-DNDC, but to date have not been validated. In this study, our objectives are to: (1) validate TFW-DNDC using field CH_4 and N_2O flux measurements; (2) apply TFW-DNDC to examine GHG emissions in TFFW under normal soil water level and soil salinity conditions; and (3) conduct scenario simulations using TFW-DNDC to examine the impacts of drought-induced salinity intrusion on CH_4 and N_2O emissions in TFFW along the Waccamaw and Savannah rivers. Our hypothesis is that the magnitude and direction of changes in CH_4 and N_2O emissions in TFFW under drought-induced salinity intrusion compared to normal scenarios would depend on site-specific geomorphologic settings, soil, and vegetation characteristics.

MATERIALS AND METHODS

Study sites

To test the hypothesis that the responses of CH_4 and N_2O emissions in TFFW to drought-induced salinity intrusion are dependent on site geomorphological, soil, and vegetation features, we selected sites along a salinity gradient from downriver in oligohaline marshes with relatively high soil salinity to upriver upper tidal forests with no salinity impact. Oligohaline marshes transitioned from TFFW over the later Holocene (Jones et al., 2017). The southeastern United States has a large distribution of TFFW, and we chose sites along the coastal floodplains of the Waccamaw River (South Carolina, USA) and the Savannah River (Georgia and South Carolina, USA) for this study (Figure 1). Four sites along each river were selected to include TFFW (Figure 1, Upper Forest, 0–0.1 psu), low-oligohaline tidal forests (Figure 1, Middle Forest, 0.5–2.1 psu), moderate-oligohaline tidal forests (Figure 1, Lower Forest, 1.7–3.9 psu), and high-oligohaline marshes (Figure 1, Marsh, 3.3–4.7 psu) (Krauss et al., 2018; Stagg et al., 2017). Tides are semi-diurnal on the Waccamaw and Savannah rivers, and tidal ranges at their mouths are 1.1 and 2.3 m, respectively (Cormier et al., 2013; Krauss et al., 2018). Wetting and drying (depth, duration, frequency) vary with local site condition including surface elevation and distance to tidal creeks and the river (Noe et al., 2013). Saltwater can reach as much as 32 km upstream under low flow conditions and 5 km upstream during normal river flow conditions along the Waccamaw River and approximately 45 km upstream during low flow conditions and approximately 13 km upstream during normal conditions along the Savannah River (Doyle et al., 2007; Duberstein & Kitchens, 2007; Krauss et al., 2018). The Savannah River, an alluvial river, typically carries red, eroded soils of the Piedmont and has higher silt and clay loads than "blackwater" rivers (Cormier et al., 2013). In contrast, the Waccamaw River is a "blackwater" river, and is characterized by a high concentration of dissolved organic matter and dark color (Ensign et al., 2013). The dominant tree species on Upper sites include *Taxodium distichum* (baldcypress), *Nyssa aquatica* (water tupelo), *Nyssa biflora* (swamp tupelo), *Acer rubrum* (red maple), and *Fraxinus spp.* (ash), while *T. distichum* and *N. biflora* are dominant at Middle sites, and *T. distichum* is dominant at Lower sites but marsh plants are invading the understory. At the oligohaline Marsh sites, dominant species include *Zizaniopsis mileacea* (giant cutgrass), *Spartina cynosuroides* (big cordgrass), *Bolboschoenus robustus* (sturdy bulrush), and *Typha latifolia* (cattail) (Ensign et al., 2013). Soils at the TFFW sites along both rivers were classified in the Typic Hydraquent family in the Soil Survey Geographic Database (SSURGO).

Model description

TFW-DNDC is a process-driven biogeochemistry model for tidal freshwater wetlands that can be used to predict impacts of increasing soil salinity due to climate change and sea level rise; specifically, it simulates the dynamics of C and N in TFFW ecosystems and assesses the

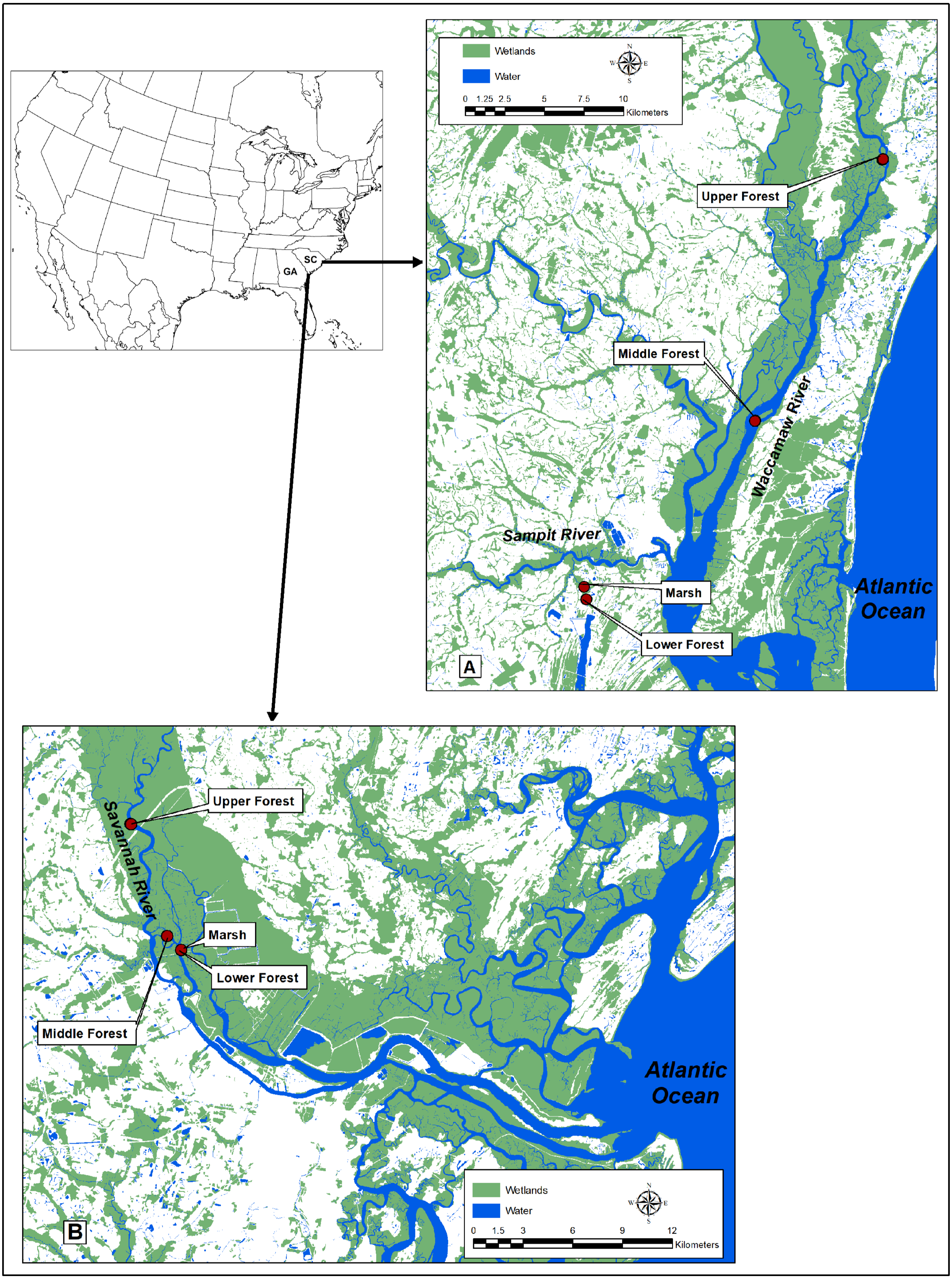

FIGURE 1 Location of the tidal freshwater forested wetlands forest and oligohaline marsh sites (red dots) along the (top right) Waccamaw River, South Carolina, and (lower) Savannah River, Georgia.

impacts of increasing salinity on plant productivity, plant and soil respiration, and SOC sequestration rate and storage (Wang, Dai, Trettin, et al., 2022). TFW-DNDC consists of five sub-models: hydrology, plant growth, soil organic matter, methanogenesis/methanotroph, and nitrification/denitrification (Figure 2). The ecological drivers of TFW-DNDC include climate, hydrology, soil, vegetation, and disturbance. Critical biogeochemical processes, including photosynthesis, plant and soil respiration, soil organic matter decomposition, N/P mineralization, nitrification, denitrification, carbon allocation, carbon storage, carbon consumption, and GHG emissions, are incorporated into TFW-DNDC. The impacts of environmental conditions such as soil salinity, light/radiation, air/soil temperature, precipitation, soil moisture, redox potential, soil pH, and nutrients on these biogeochemical transformations are simulated. Major processes involved in GHG emissions include soil organic matter decomposition, methanogenesis, methanotrophy, nitrification, and denitrification (Cui et al., 2005; Dai et al., 2018a; Li et al., 2004; Wang, Dai, Trettin, et al., 2022; Zhang et al., 2002).

Soil redox potential (Eh) is one of the critical drivers that determine the rates of decomposition, nitrification, denitrification, and methanogenesis that, as a net influence, produce CO_2, N_2O, and CH_4 fluxes. When the soil is saturated due to flooding, oxygen is depleted in the soil and leads to anoxic conditions (Eh normally in the range of −300 to 0 mV), resulting in reductive reactions such as denitrification or methanogenesis. In contrast, when the soil is under oxic conditions (Eh normally in the range between 100 and 650 mV), oxidative reactions such as decomposition, nitrification, and methane oxidation will occur. Soil Eh in TFW-DNDC is determined by concentrations of existing oxidants and reductants in the soil liquid phase (Li et al., 2004).

Soil organic matter (SOM: litter, microbes, humics) is divided into very labile, labile, and resistant pools. SOM decomposition is simulated with first-order kinetics with controlling factors including soil salinity, soil temperature, moisture, nitrogen availability, soil texture, and specific decomposition rates of the SOM pools. Decomposition can take place under both oxic and anoxic conditions. Salinity

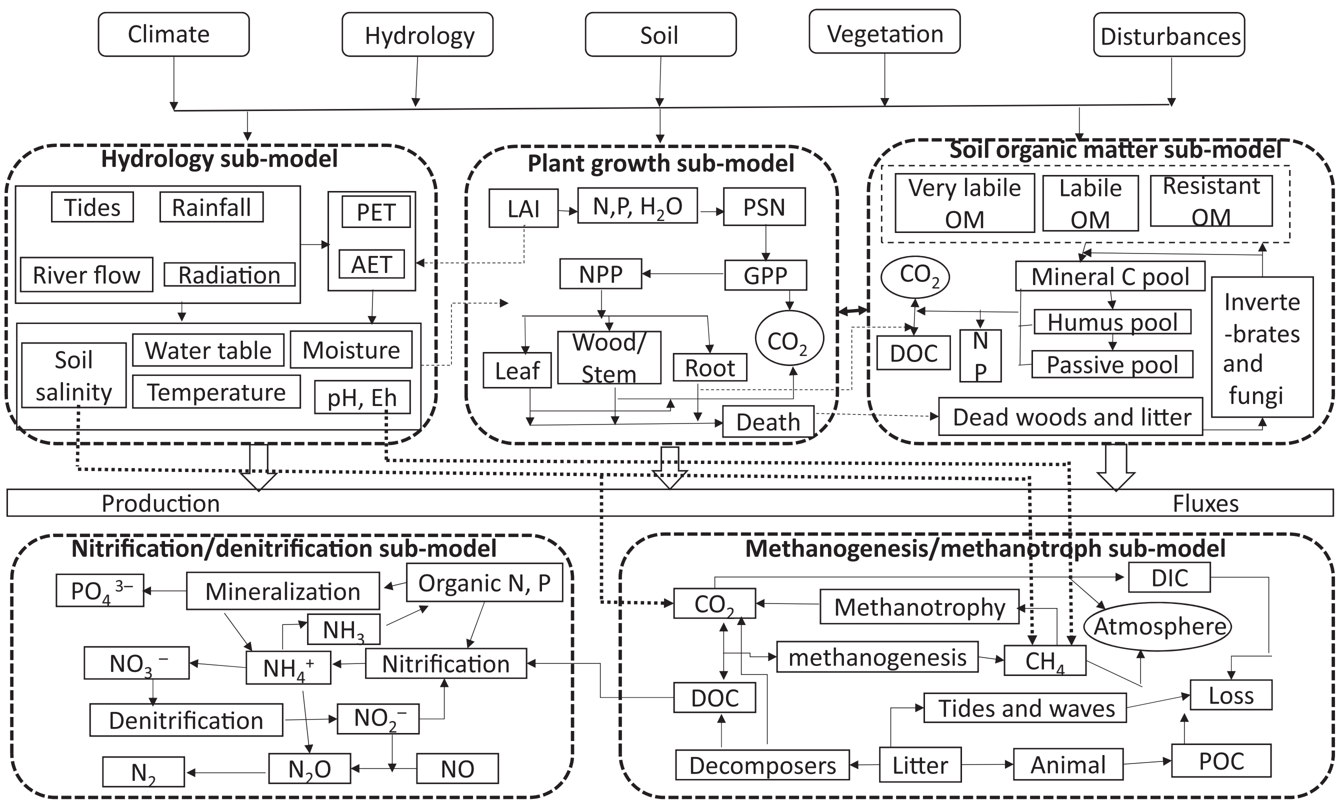

FIGURE 2 Conceptualization of Tidal Freshwater Wetland DeNitrification-DeComposition (TFW-DNDC) (Wang, Dai, Trettin, et al., 2022) that was modified from the Mangrove Carbon Assessment Tool DeNitrification-DeComposition model (MCAT-DNDC) (Dai et al., 2018a). Modifications for the impacts of soil salinity on decomposition and methane emission and the impact of redox potential (Eh) on methane emission were indicated by the dashed lines with arrow. AET, actual evapotranspiration; DIC, dissolved inorganic carbon; DOC, dissolved organic carbon; Eh, redox potential; GPP, gross primary productivity; LAI, leaf area index; NPP, net primary productivity; PET, potential evapotranspiration; POC, particulate organic carbon; PSN, photosynthesis.

affects SOM decomposition in tidal wetlands including TFFW and oligohaline marshes (Luo et al., 2019; Morrissey et al., 2014; Weston et al., 2011). A negative relationship between soil salinity and decomposition rate, as discerned using an in situ litterbag experiment on native roots on all sites along both rivers, was used (Stagg et al., 2017) and converted to a salinity limiting factor in TFW-DNDC using the following formula:

$$f_{\text{somsalt}} = -0.0755s + 1.0377, \quad \text{when} \quad s \geq 0.5; \qquad f_{\text{somsalt}} = 1 \quad \text{when} \quad s < 0.5, \tag{1}$$

where f_{somsalt} is salinity effect on soil organic matter decomposition, s is soil salinity in psu.

For methanogenesis and methanotrophy, effects of soil salinity, sulfate reduction, iron oxide formation, manganese availability, water table, and tides/sulfate concentration on CH_4 production, consumption, and transport processes are simulated. The change of CH_4 content is the difference between production and oxidation, including diffusion between soil layers or to the atmosphere, emissions through ebullition, and plant-mediated CH_4 transport (Cheng et al., 2018; Reddy & DeLaune, 2008). Methane production is also a function of carbon substrates, temperature, pH, and redox potential (i.e., produced only when Eh is below −150 mV, Li et al., 2004). Anaerobic oxidation of methane (AOM) with sulfate, nitrate, and nitrite reduction (Dai et al., 2018a) is modeled for tidal wetlands with salinity intrusion since high rates of AOM in freshwater wetlands often occur (Segarra et al., 2015). Segarra et al. (2015) found that AOM in freshwater wetlands may reduce methane emissions by over 50%. CH_4 oxidation (methanotrophy) is mainly controlled by CH_4 concentration, redox potential, temperature, and concentration of oxidants including SO_4^{2+}, NO_3^-, and NO_2^- and oxygen in TFW-DNDC. Methanotrophy can be significant in TFFW (Megonigal & Schlesinger, 2002), with lesser-known influences down-estuary, but provides an important potential Eh-mediated feedback mechanism to limit net CH_4 emissions despite being a freshwater habitat. Methanotrophic bacteria are capable of growing on multiple or singular carbon substrates ("facultative methanogens"; Theisen & Murrell, 2005), but prominently target CH_4 under aerobic conditions while living facultatively with or without oxygen (Hanson & Hanson, 1996), and therefore proliferate in TFFW characterized by alternating periods of oxygenation. CH_4 diffusion is also controlled by soil water content and water table height and occurs when the water table is below the soil surface (Walter & Heimann, 2000), including in tidal forest-to-marsh transitions (Kelley et al., 1995). Ebullition occurs when the soil water table is above soil surface and soil CH_4 concentration exceeds a threshold of 750 μmol L^{-1} (Walter & Heimann, 2000). Plant-mediated transport is determined by CH_4 concentration, plant aerenchyma (Frenzel & Rudolph, 1998), and soil pore space. For tidal marshes, it was found that oligohaline systems (0.5–5 psu) have significantly higher CH_4 emissions than mesohaline (5–18 psu) and even freshwater marshes (0–0.5 psu) (Liu et al., 2019; Poffenbarger et al., 2011; Wang et al., 2017). Poffenbarger et al. (2011) indicated that there is still a decreasing trend of CH_4 emission with increase in salinity from freshwater to mesohaline wetlands. However, the slope of the linear regression relationship may be less for purely fresh systems (or slowed decreasing), spiked statistically by the occurrence of higher and more variable CH_4 emissions in the 0.5–5 salinity range (Liu et al., 2019; Poffenbarger et al., 2011; Wang et al., 2017). Thus, we modified the negative linear relationship between soil porewater salinity and methane flux in MCAT-DNDC of Dai et al. (2018a) based on our TFFW field data (Krauss & Whitbeck, 2012) and consideration that relatively higher CH_4 emissions in the salinity range of 5.0–7.5 psu (Liu et al., 2019; Poffenbarger et al., 2011; Wang et al., 2017) would be simulated by TFW-DNDC compared to the mangrove habitat-validated MCAT-DNDC. For TFW-DNDC, we determined the following relationship:

$$f_{CH_4\text{salt}} = e^{\left(\frac{-\varphi s^2}{10}\right)} \quad \text{when} \quad s \geq 0.5; \qquad f_{CH_4\text{salt}} = 1 \quad \text{when} \quad s < 0.5, \tag{2}$$

where $f_{CH_4\text{salt}}$ is salinity effect on methane production, φ is a coefficient and calibrated to the optimal value of 0.95, s is soil salinity in psu. It should be noted that Equation 2 can be only used for low salinity sites. When salinity ≥10, f is approximately zero because of an exponential decrease with an increase in salinity.

In this study, we adopted the Eh limiting factor from Cheng et al. (2018) with a modification to the threshold of −150 to −300 mV. Field measurements of Eh from Savannah sites at 15 and 30 cm soil depths during dry (August 2006 and August 2007) and wet sampling periods (November 2006 and March 2007) showed that Eh at our sites ranges from −300 to 250 mV, and CH_4 emission tended to substantially decrease at 250 mV for tidal swamps (Yu et al., 2006). The effect of Eh on methane production (f_{E_h}) is modified as following:

$$f_{E_h} = e^{\left(-1.7\left(\frac{300+E_h}{300}\right)\right)} \quad \text{when} \quad 250 > E_h > -300; \qquad f_{E_h} = 1 \quad \text{when} \quad E_h < -300; \qquad f_{E_h} = 0 \quad \text{when} \quad E_h > 250. \tag{3}$$

For nitrification, under oxic conditions, ammonium (NH_4^+) is oxidized to nitrate (NO_3^-) or absorbed by clay particles or transformed into ammonia (NH_3). NO or N_2O can be evolved as byproducts, all of which were verified to be in range for TFFW and transitional habitat for the same Waccamaw and Savannah sites (Noe et al., 2013) that are being simulated by TFW-DNDC. In the model, nitrification rate is regulated by soil temperature, moisture, Eh, and pH as well as concentrations of dissolved organic carbon (DOC) and NH_4^+. For denitrification, under anoxic conditions, nitrate (NO_3^-) is reduced to NO_2^-, NO, N_2O, and N_2. Denitrification rate is regulated by soil temperature, pH, and Eh, as well as the concentrations of substrates such as DOC. Denitrification is also the predominant mechanism of nitrate removal, with very limited N_2O flux contributions from the byproduct of NH_4 nitrification (sensu Freeman et al., 1997). CO_2 is also produced through denitrification.

For details about TFW-DNDC equations that describe these processes and critical model parameters, refer to Wang, Dai, Trettin, et al. (2022), Dai et al. (2018a), Li et al. (2000), Li et al. (2004), and Zhang et al. (2002). TFW-DNDC is written in C/C++ and operates on a daily time step with summation to annual output. A spin up period of 2 years was adopted to reduce the influences of initial conditions (primarily soil salinity and water level) and numerical calculations on model stability (Wang, Dai, Trettin, et al., 2022). Soil depth in this study was simulated to 50 cm below the soil surface. Age of organic matter was of recent deposition at the soil surface (Noe et al., 2016), but up to 144 years old (Savannah River Marsh) to 1046 years old (Waccamaw River Lower) at the 50 cm soil depth across all sites (Krauss et al., 2018).

Input data

Input data to run TFW-DNDC include site-specific geographical location (latitude, longitude), elevation, vegetation, soil, and time-series of climate (daily precipitation, maximum and minimum temperature), and hydrology (soil water level and soil salinity). Major site-specific location, elevation, and vegetation data and soil data for model simulations are shown in Tables 1 and 2, respectively. Daily temperature and rainfall at the forest and marsh sites along the two rivers were obtained from the Oak Ridge National Laboratory's Daily Surface Weather and Climatological Summaries (Daymet) database (Thornton et al., 2022). Data on daily soil water level at these TFFW sites were derived from in situ measurements of hourly water level (2004–2016) and surface elevation (Cormier et al., 2013; Krauss et al., 2009). Daily soil porewater salinity for these sites was derived from a mass balance-based hydrological model (Wang et al., 2020a, 2020b). Critical model parameters for TFW-DNDC were obtained from the DNDC modeling literature (Cui et al., 2005; Dai et al., 2018a; Li et al., 2000, 2004; Zhang et al., 2002). These model parameters include intercept of the relationship between maximum photosynthetic rate and foliar N; maximal net photosynthetic rate; maximum, minimum, and optimal temperature for photosynthesis; growth and maintenance respiration fraction; temperature factor on leaf respiration (Q_{10}); leaf area index; accumulative thermal degree days for starting leaf and wood growth; accumulative thermal degree days for ceasing leaf and wood growth; and a water use efficiency constant. The values of these critical model parameters can be found in tab. S1 in appendix S2 of Wang, Dai, Trettin, et al. (2022).

Model validation

TFW-DNDC was previously calibrated and validated against field observations for both Savannah River and Waccamaw River sites using local ecological drivers for

TABLE 1 Site-specific geographical and major vegetation data used in Tidal Freshwater Wetland DeNitrification-DeComposition (TFW-DNDC).

	Savannah				Waccamaw			
Characteristic	**Upper**	**Middle**	**Lower**	**Marsh**	**Upper**	**Middle**	**Lower**	**Marsh**
Latitude (° N)	32.2387	32.1757	32.1673	36.1672	33.5552	33.4225	33.3400	33.3500
Longitude (° W)	81.1563	81.1442	81.1369	81.1364	79.0897	79.2074	79.3421	79.3449
Elevation (m, NAVD88)	1.21	1.12	1.19	1.24	0.74	0.56	0.37	0.36
Initial leaf mass (kg C ha^{-1})	3092.0	1722.0	843.0	2250.0	3092.0	1722.0	843.0	2250.0
Initial wood mass (kg C ha^{-1})	2830.0	580.0	349.0		2830.0	580.0	349.0	
Initial root mass (kg C ha^{-1})	1368.0	4110.0	3743.0	3825.0	1368.0	4110.0	3743.0	3825.0
Leaf N concentration (%)	1.26	1.12	1.41	1.40	2.42	1.17	1.03	1.40
Foliar C/N ratio	39.6	45.8	36.0		36.0	46.0	51.0	
Foliar N/P ratio	10.5	10.0	15.0		10.5	10.0	15.0	

Note: Sources for data: geographical location and elevation: Wang et al. (2020a); vegetation feature: Krauss et al. (2009), Cormier et al. (2013), Conner et al. (2014).

TABLE 2 Major site-specific soil data used in Tidal Freshwater Wetland DeNitrification-DeComposition (TFW-DNDC).

	Savannah				Waccamaw			
Characteristic	**Upper**	**Middle**	**Lower**	**Marsh**	**Upper**	**Middle**	**Lower**	**Marsh**
SOC concentration (kg C kg^{-1})	0.13	0.14	0.05	0.06	0.17	0.13	0.19	0.10
Initial total SOC (kg C ha^{-1})	305,900	143,200	369,400	122,600	60,100	159,500	225,300	386,100
Total P (g P kg^{-1})	0.70	0.82	1.44	1.34	0.86	0.73	0.53	0.80
pH	5.2	5.0	5.0	4.7	5.3	4.7	4.6	4.0
Bulk density (g cm^{-3})	0.26	0.25	0.39	0.30	0.21	0.24	0.32	0.28
Saturated hydrological conductivity (cm h^{-1})	0.02	0.02	0.05	0.07	0.03	0.03	0.07	0.07
Porosity (ratio)	0.91	0.91	0.85	0.89	0.91	0.91	0.88	0.89
Field capacity (ratio)	0.45	0.45	0.44	0.43	0.42	0.42	0.35	0.43
Wilting point (ratio)	0.27	0.27	0.22	0.22	0.22	0.22	0.11	0.22
Clay fraction (%)	45.0	41.0	29.0	39.0	29.0	29.0	22.0	27.0

Note: Data sources: Ensign et al. (2013), Noe et al. (2013, 2016), Jones et al. (2017), Krauss et al. (2018), Wang et al. (2020a).

assessing annual litterfall, wood growth, root growth, plant respiration, and soil organic carbon storage (Wang, Dai, Trettin, et al., 2022). To ensure that TFW-DNDC is capable of simulating temporal (daily) variations in CH_4 and N_2O emissions across the various TFFW sites, model validation was also conducted by comparing simulated daily CH_4 and N_2O emissions with observed values. Field GHG flux data were available only for Savannah River forest sites for model validation. At each of the three forest sites along the Savannah River (upper, middle, and lower), hourly CH_4 and N_2O fluxes were calculated for samples collected at six locations 24 times from 26 October 2005 to 18 December 2007 using the static chamber method (Krauss & Whitbeck, 2012; Yu et al., 2008). At each site, all six white-plastic 29.4 × 29.4 × 30.5 cm soil chambers were darkened during measurements to moderate temperature fluctuations during the 60-min sampling periods. Gas flux data during 2006 and 2007 were used for model validation. Hourly fluxes were converted to daily rates by multiplying by 24 assuming the hourly rates represent the fluxes of the sampling days. It should be noted that, since samples were collected when water levels were less than 3 cm above the soil surface (Krauss & Whitbeck, 2012), the field hourly-measurement-determined daily CH_4 and N_2O fluxes on days with water level greater than 3 cm were not used in model validation, since the water conditions during hourly measurements were not representative of daily water level conditions. In addition, soil uptake of CH_4 and N_2O (e.g., due to lower gas concentration in soil than atmosphere) were measured on some sampling dates using darkened chambers during measurements (Krauss & Whitbeck, 2012), but uptake of N_2O was not included (CH_4 uptake was included) in the biogeochemistry model due to the lack of understanding of the uptake mechanisms (Krauss & Whitbeck, 2012). Therefore, measurements of negative N_2O fluxes were removed from comparison with simulations, noting that overall N_2O fluxes did not differ significantly from 0 on the Savannah River forested wetland sites (Krauss & Whitbeck, 2012) or in a swamp forest-adjacent tidal freshwater marsh in Louisiana (Krauss et al., 2016). Due to a skewed distribution in measured CH_4 and N_2O fluxes, median or mode rather than the arithmetic mean of the measurements were considered more representative and used to evaluate model performance.

The performance of TFW-DNDC was evaluated using the coefficient of determination (R^2, squared correlation coefficient), bias, and root mean square error (RMSE). The coefficient of determination measures the linear association between modeled and observed data; a high correlation coefficient is considered desirable. Typically values greater than 0.5 are considered acceptable. Bias is the average of the difference between modeled and observed values; a good model exhibits low bias. RMSE describes the residual difference between model performance and actual data; a good model has low RMSE values. Values for R^2, bias, and RMSE are calculated as:

$$R^2 = \left(\frac{\sum (O_i - \overline{O})(P_i - \overline{P})}{\sqrt{\sum (O_i - \overline{O})^2} \sqrt{\sum (P_i - \overline{P})^2}} \right)^2, \tag{4}$$

$$\text{bias} = \frac{\sum (P_i - O_i)}{n}, \tag{5}$$

$$\text{RMSE} = \sqrt{\frac{\sum (P_i - O_i)^2}{n}}, \tag{6}$$

where O_i *and* P_i are observed and simulated values at each time i; $\overline{O}$ and $\overline{P}$ are observed mean and simulated mean; n is the number of observations.

Scenario analysis

The validated TFW-DNDC was used to examine trends and variability in CH_4 and N_2O emissions at the Waccamaw and Savannah forest and oligohaline marsh sites under normal and drought conditions. Normal years and dry years in this study were determined by the Palmer Drought Severity Index (PDSI) for the Northeast Division of South Carolina and Southeast Division of Georgia, historical river discharge data (1994–2017 for Waccamaw sites and 2008–2017 for Savannah sites), and in situ soil water level data relative to soil surface during 2010–2016 (Cormier et al., 2013; Wang et al., 2020a, 2020b). The characteristics of soil salinity and water level under the normal and drought conditions in soils of the TFFW sites along the two rivers are shown in Table 3.

Statistical analysis

The impacts of drought-induced saltwater intrusion on simulated CH_4 and N_2O emissions at the TFFW sites along the two river systems were analyzed using a three-way analysis of variance (ANOVA) with river, site, and drought and their interactions as explanatory variables, and two-way ANOVAs with site and drought and their interaction as explanatory variables. When necessary, the simulation results were transformed using the Box-Cox method prior to analysis to meet normality and homoscedasticity assumptions. Whenever a significant interaction effect was detected via two-way ANOVAs, a series of one-way ANOVAs were used to analyze individually the impact of drought-induced saltwater intrusion on CH_4 and N_2O emissions at each of the TFFW sites. All post hoc tests were performed using Tukey's HSD. The SAS 9.3 software package (SAS Institute, Cary, North Carolina, USA) was used for the statistical analyses. All the tests were two-tailed based on type III sums of squares and considered significant at $p < 0.05$.

RESULTS

Model validation

TFW-DNDC produced fluxes of CH_4 and N_2O were within the ranges of observed values at the upper, middle, and lower forest sites along the Savannah River (Figures 3 and 4). Model simulations of daily CH_4 and N_2O fluxes showed good agreements with field observations (R^2 0.54 for CH_4 and 0.75 for N_2O), although the model tended to overestimate CH_4 emissions (bias = 0.004, RMSE = 0.026 kg C ha^{-1} day^{-1}) (Figure 3), whereas it tended to underestimate fluxes of N_2O (bias = −0.84, RMSE = 1.74 g N ha^{-1} day^{-1}) (Figure 4). Overall, model validation suggests that TFW-DNDC is capable of simulating CH_4 and N_2O emissions in tidal forested wetlands with reasonable accuracy considering the complexity of the biogeochemical processes involved and the large spatial (across sites and within sites) and temporal variations in CH_4 and N_2O fluxes reflected by field data.

Drought-induced salinity intrusion on CH_4 and N_2O emissions

There were significant "river by site by scenario" ($p < 0.0001$) and "site by scenario" ($p < 0.05$) interactions

TABLE 3 Summary statistics of water level and soil salinity and water level under the normal and drought conditions in the upper, middle, and lower forest and oligohaline marsh sites along the Savannah River and the Waccamaw River.

Site	Savannah		Waccamaw	
	Normal (2010)	Dry (2012)	Normal (2013)	Dry (2012)
Water level (cm)				
Upper	−2.41 ± 7.62	−3.02 ± 4.55	0.46 ± 5.61	−2.34 ± 4.69
Middle	0.77 ± 6.23	−2.18 ± 6.92	3.41 ± 5.34	0.57 ± 6.24
Lower	4.64 ± 5.82	−9.88 ± 9.05	6.70 ± 5.52	6.23 ± 6.00
Marsh	10.23 ± 6.08	−0.85 ± 3.71	10.36 ± 6.01	9.93 ± 6.11
Soil salinity (psu)				
Upper	0.10 ± 0.00	0.10 ± 0.00	0.10 ± 0.00	0.10 ± 0.00
Middle	1.09 ± 0.74	2.37 ± 0.37	0.63 ± 0.57	0.78 ± 0.53
Lower	3.46 ± 2.12	7.23 ± 0.72	1.91 ± 1.14	6.45 ± 0.08
Marsh	3.63 ± 2.40	7.61 ± 1.38	2.10 ± 1.44	4.98 ± 0.38

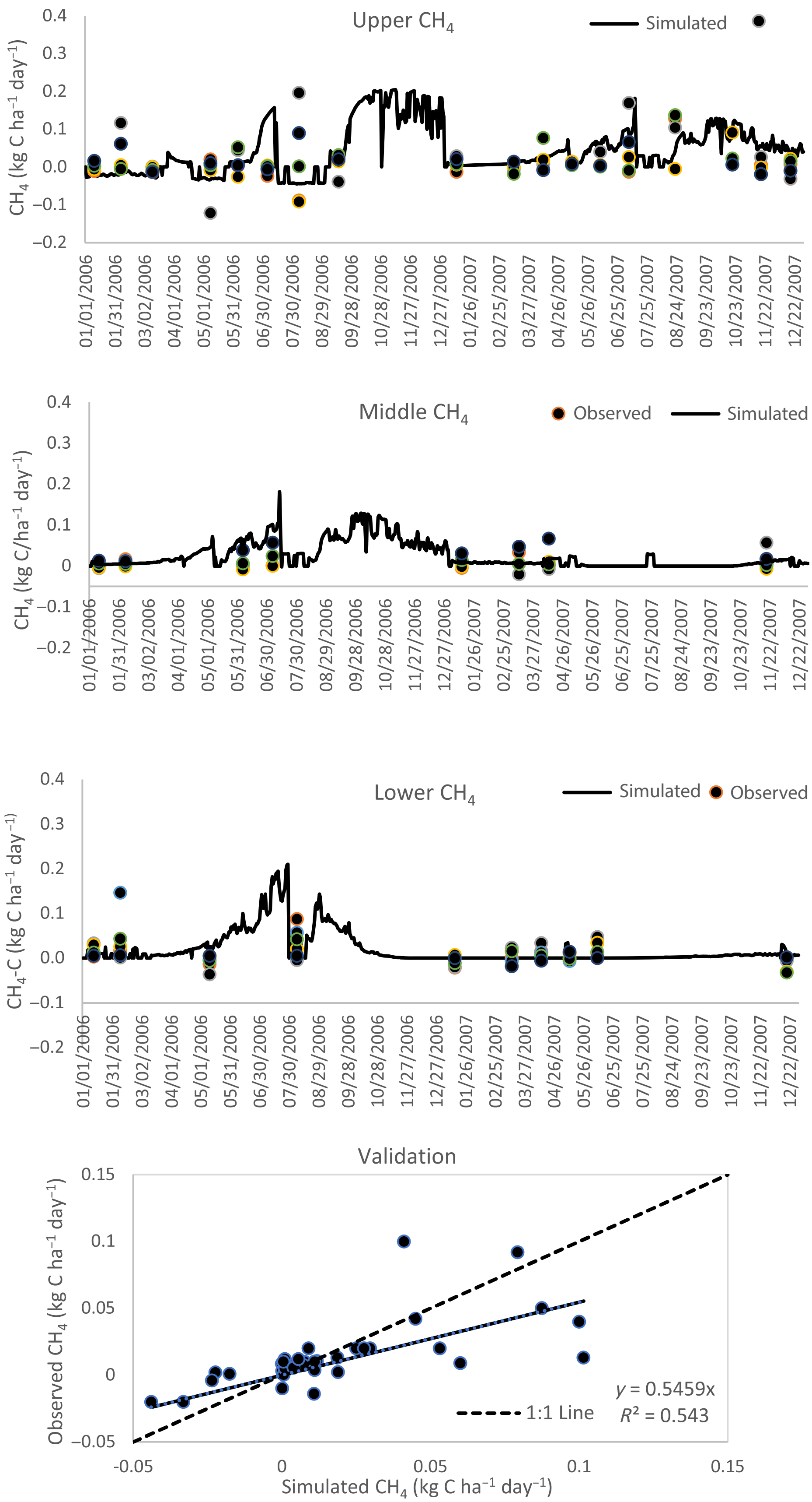

FIGURE 3 Comparisons between simulated and observed methane (CH_4) emissions at the upper, middle, and lower (top three panels, respectively) forest sites along the Savannah River. Model performance on CH_4 emissions was evaluated by comparing simulated and observed fluxes with R^2 for the fitted regression line (lower panel).

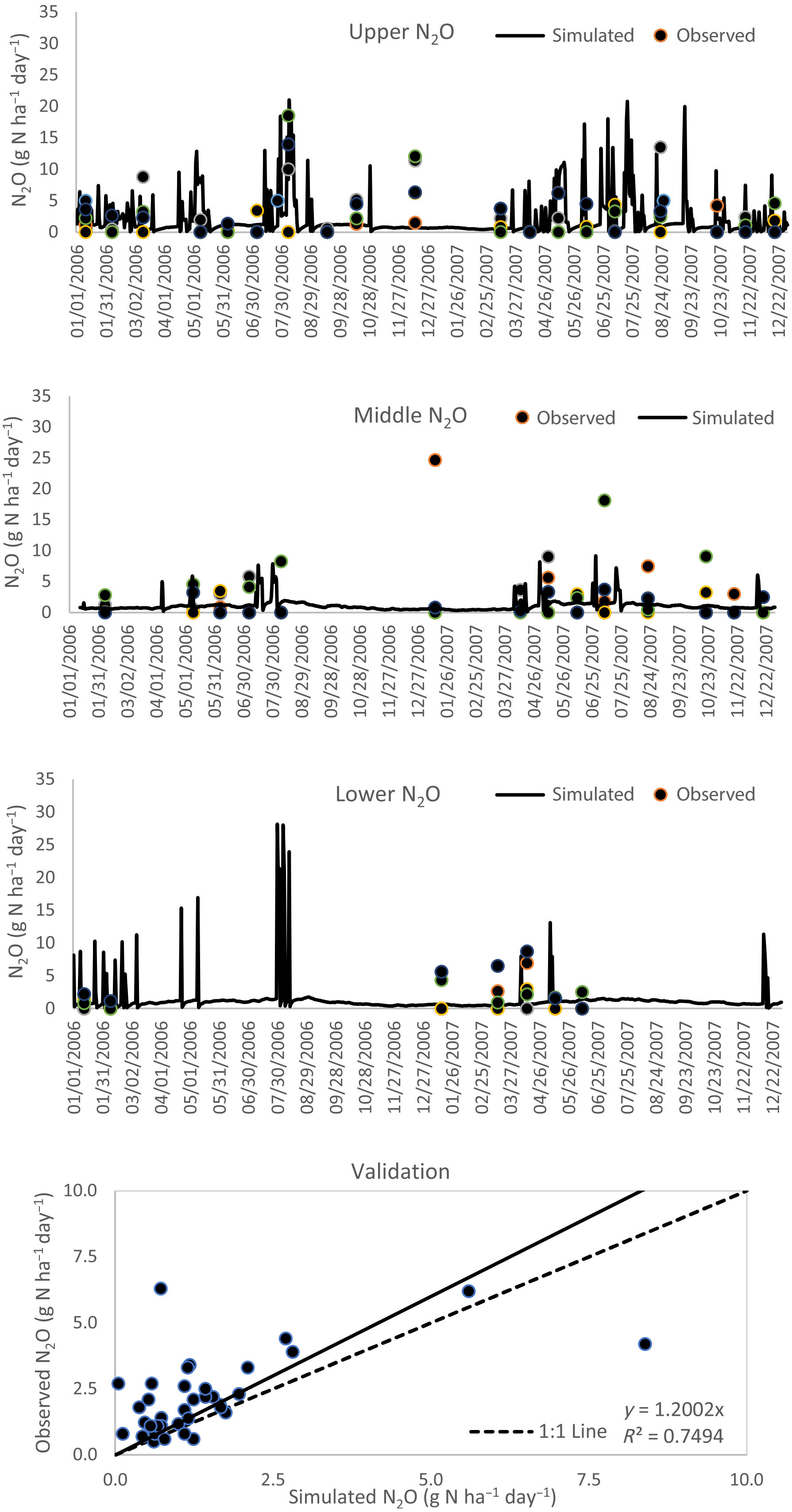

FIGURE 4 Comparisons between simulated and observed nitrous oxide (N_2O) emissions at the upper, middle, and lower (top three panels, respectively) forest sites along the Savannah River. Model performance on N_2O emissions was evaluated by comparing simulated and observed fluxes with R^2 for the fitted regression line (lower panel).

for simulated CH_4 and N_2O fluxes (Appendix S1: Tables S1 and S2, simulation results are available in Wang, Dai, Krauss, et al., 2022), indicating that drought-induced saltwater intrusion significantly affected the emissions of CH_4 and N_2O, and the responses of CH_4 and N_2O emissions to drought-induced saltwater intrusion varied significantly by river system (the Savannah and Waccamaw rivers) and by TFFW study site location along rivers (upper, middle, lower, and marsh). One-way ANOVAs (Appendix S1: Table S3) revealed that the increase in soil salinity and reduction in soil water level due to drought and drought-induced saltwater intrusion tended to greatly affect CH_4 and N_2O emissions in TFFW, and the impacts of drought-induced saltwater intrusion would vary with the river systems and site geomorphologic settings to determine the magnitude and direction of the biogeochemical processes in responses to drought-induced saltwater intrusion.

Along the Savannah River, simulated annual CH_4 fluxes increased significantly ($p < 0.0001$, Appendix S1: Table S3) in the upper forest from 56.37 kg C ha^{-1} year^{-1} under the normal condition to 144.25 kg C ha^{-1} year^{-1} under the drought condition, an increase of 156% (Figure 5). In contrast, simulated CH_4 fluxes decreased significantly (all $p < 0.0001$, Appendix S1: Table S3) in the middle (by 26.51 kg C ha^{-1} year^{-1}, −50%), lower (by 17.18 kg C ha^{-1} year^{-1}, −213%), and oligohaline marsh (by 2.72 kg C ha^{-1} year^{-1}, −137%) sites, respectively (Figure 5). As expected, there was a decreasing trend of CH_4 emissions along the upper, middle, lower, and oligohaline marsh gradient under both normal and drought conditions (Figure 5). Methane tended to emit year-round in the upper and middle forest sites with daily highest CH_4 fluxes as high as 0.76 kg C ha^{-1} day^{-1} and 1.10 kg C ha^{-1} day^{-1} under normal and drought conditions in the upper forest site, respectively, and 0.38 kg C ha^{-1} day^{-1} and 0.16 kg C ha^{-1} day^{-1} in the middle forest site, respectively (Figure 6). Methane emissions in the upper forest site were inhibited in summer months under both scenarios. Unlike the upper and middle forest sites, in the lower and oligohaline marsh sites CH_4 emissions were low and uptake of CH_4 occurred during the normal condition; CH_4 was emitted at <0.1 kg C ha^{-1} day^{-1} mostly in the spring and summer under the drought condition (Figure 6).

Simulated N_2O emissions were affected significantly (all $p < 0.01$) by the drought-induced saltwater intrusion in all but the upper forest sites ($p = 0.53$, Appendix S1: Table S3). Simulated annual N_2O fluxes increased significantly from 0.19 kg N ha^{-1} day^{-1} under the normal condition to 1.09 kg N ha^{-1} day^{-1} under the drought condition in the lower forest site (+474%), and from 0.04 kg N ha^{-1} day^{-1} under the normal condition to 0.11 kg N ha^{-1} year^{-1} under the drought condition in the oligohaline marsh site (+175%), respectively (Figure 5). In contrast, simulated

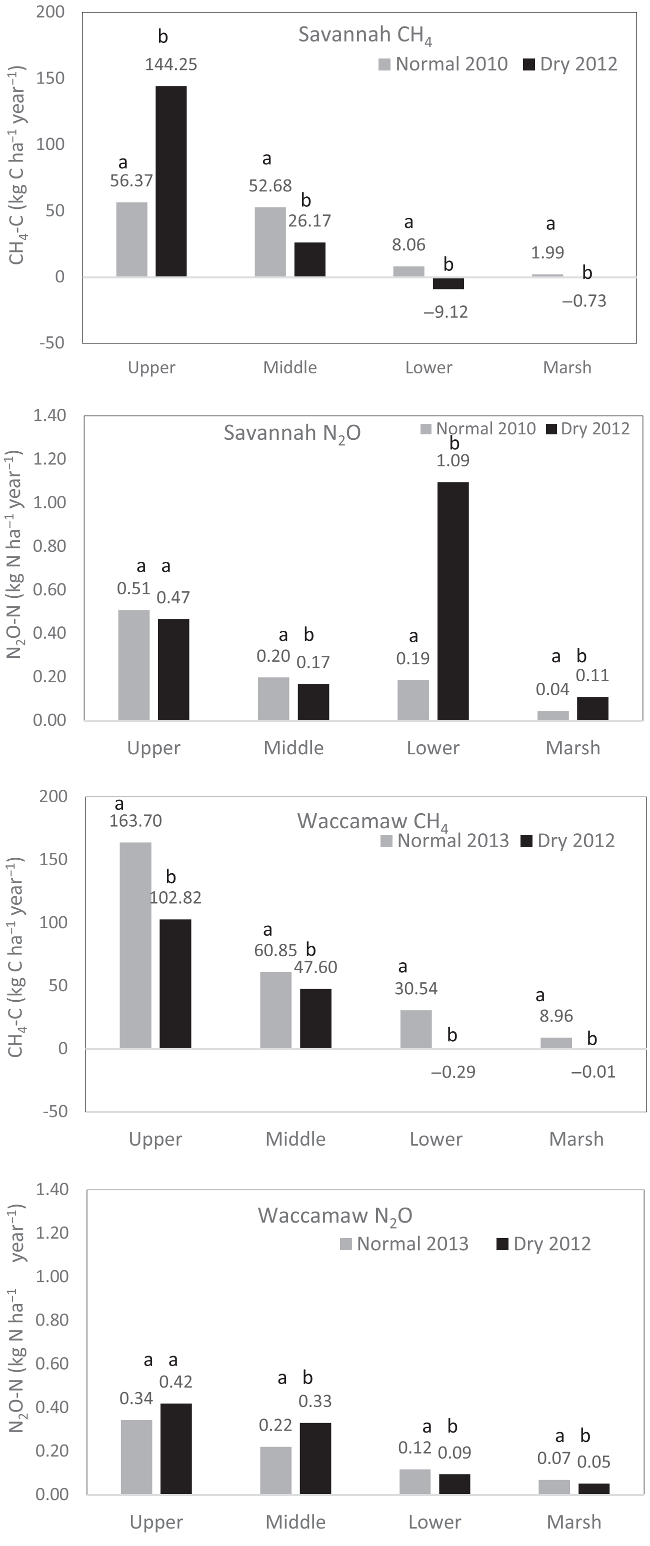

FIGURE 5 Simulated annual CH_4 (top and third panels) and N_2O (second and fourth panels) emissions under the normal and drought conditions at the upper, middle, and lower forest and oligohaline marsh sites along the Savannah and Waccamaw rivers. Same letters (i.e., "a a") indicate that there is no significant difference in CH_4 and N_2O fluxes between normal and drought conditions while different letters (i.e., "a b") indicate significant differences in fluxes between the two conditions.

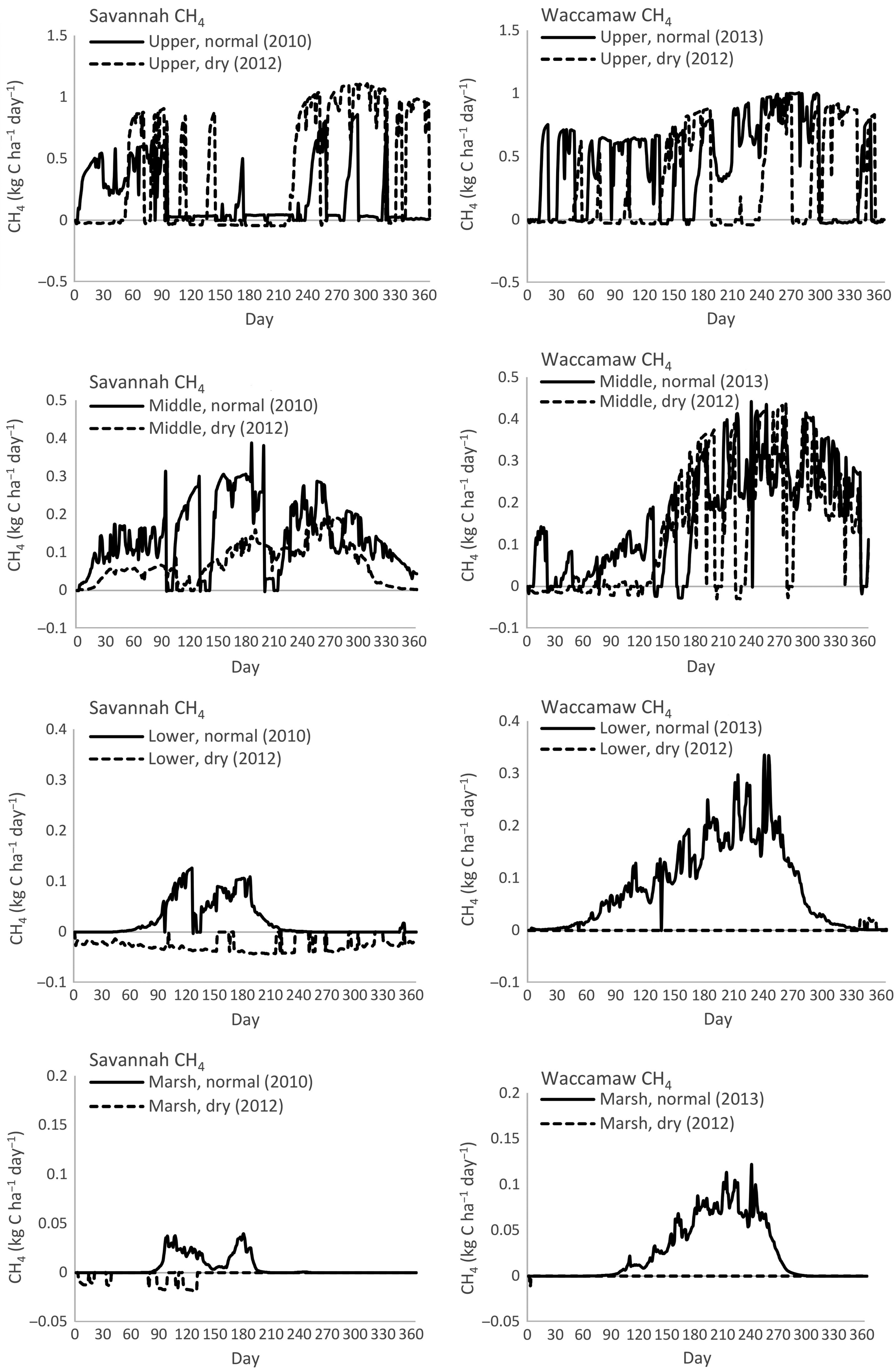

FIGURE 6 Simulated daily CH_4 emissions under the normal and drought conditions at the upper (top row), middle (second row), and lower (third row) forest and oligohaline marsh (fourth row) sites along the Savannah and Waccamaw rivers.

annual N_2O fluxes in the middle forest site decreased significantly (−15%) from 0.2 kg N ha^{-1} $year^{-1}$ under the normal condition to 0.17 kg N ha^{-1} $year^{-1}$ under the drought condition (Figure 5). The simulated daily N_2O fluxes over the year showed that the decreases in the middle forest site occurred mostly in spring and summer when peaks in N_2O emission occurred in the normal condition (Figure 7). Unlike the middle forest site, an increase in simulated daily N_2O fluxes under the drought condition in the oligohaline marsh site was caused by the increased emission peaks during spring and one in the late fall, whereas the increase in N_2O fluxes in the lower forest site were associated with increased peaks throughout the year (Figure 7).

Along the Waccamaw River, simulated annual CH_4 emissions under the drought condition decreased significantly (all $p < 0.001$, Appendix S1: Table S3) in the upper, middle, lower, and oligohaline marsh sites compared to the normal condition (Figure 5). The simulated CH_4 fluxes decreased significantly in the upper (by 60.88 kg C ha^{-1} $year^{-1}$, −37%), middle (by 13.25 kg C ha^{-1} $year^{-1}$, −22%), lower (by 30.83 kg C ha^{-1} $year^{-1}$, −101%), and oligohaline marsh (by 8.97 kg C ha^{-1} $year^{-1}$, −100%) sites. Similar to the seasonal patterns and the magnitude in CH_4 emission in the Savannah upper and middle forest sites, CH_4 was also emitted year-around for the Waccamaw upper and middle forest sites. A difference in CH_4 emissions between the two middle forest sites is that large CH_4 emissions tended to occur during summer under the normal condition for Savannah middle forest, whereas peak CH_4 emissions occurred in fall season under both normal and drought conditions for Waccamaw middle forest (Figure 6). There were very little CH_4 emissions and some uptake in the lower and marsh sites, occurring mostly during late spring and early fall under the normal condition, and CH_4 emissions tended to be completely inhibited under the drought conditions (Figure 6).

Simulated N_2O emissions were also affected significantly (all $p < 0.05$) by the drought-induced saltwater intrusion in all but the upper forest sites along the Waccamaw River ($p = 0.20$, Appendix S1: Table S3). The impacts of drought-induced saltwater intrusion at the Waccamaw sites were opposite of those at the Savannah sites. Simulated annual N_2O fluxes increased significantly in the middle forest site (+50%) but decreased significantly in the lower forest (−25%) and oligohaline marsh (−28.6%) sites, respectively, along the Waccamaw River (Figure 5). The increase in N_2O emissions in the middle forest site was reflected by the increases in daily emission peaks throughout the year (Figure 7). The decrease in N_2O emissions under the drought condition was reflected by the reduced emissions during most of the year, although increases in the wintertime did occur for the lower forest site while N_2O emissions were found to be reduced throughout the year for the marsh site (Figure 7). At the oligohaline marsh sites of both rivers, N_2O fluxes were significantly lower than the forest sites.

DISCUSSION

Model performance and limitations

Model validation showed that TFW-DNDC tended to overestimate CH_4 emissions while it tended to underestimate fluxes of N_2O at tidal freshwater forest sites along the Savannah River where field measurements were available. There are multiple reasons that may help explain the discrepancies between modeled and observed CH_4 and N_2O fluxes. First, there are large within-site spatial variations in CH_4 and N_2O fluxes during the time of measurements especially at the upper forest site. For example, at the upper forest site in July 2006, CH_4 fluxes ranged from ~ −0.1 (uptake) to 0.2 (emission) kg CH_4-C ha^{-1} day^{-1} and N_2O fluxes ranged between 0 and 18 g N_2O-N ha^{-1} day^{-1}, respectively (Figures 3 and 4). Such large variations in CH_4 and N_2O fluxes could be attributed to the within-site differences in microtopography, soil moisture, surface vegetation cover, soil organic matter content, and soil texture, since even small differences in these site-level conditions may cause large changes in biogeochemical responses. For example, CH_4 fluxes were significantly lower in soils of hummock than in tidal forest hollows, or small depressional areas between trees (Minick, Mitra, et al., 2019; Yu et al., 2006). Furthermore, denitrification and N_2O flux potentials were found to be higher in hummocks with wet-dry fluctuation than in hollows with no fluctuation (Korol & Noe, 2020). Although our field replicates for CH_4 and N_2O fluxes were not selected by distinct hummock and hollow, such local variations in site elevation were still very likely (e.g., Duberstein & Conner, 2009), resulting in large within-site biogeochemical differentiation.

Second, field derived daily CH_4 fluxes might be overestimated, since samples using the chamber technique were collected during midday (1000–1600) when CH_4 fluxes could be inherently higher (Krauss et al., 2016; Krauss & Whitbeck, 2012) compared to simulated daily average fluxes. In other wetlands, the timing of the diurnal peak can depend on water table depth or saturation conditions (Bansal et al., 2018). It was found that chamber-based CH_4 fluxes could be 2–4 times higher than measurements from eddy covariance techniques, which provide continuous and relatively accurate flux measurements over large spatial scales (Holm et al., 2016; Krauss et al., 2016). Third, there are biases in integrating

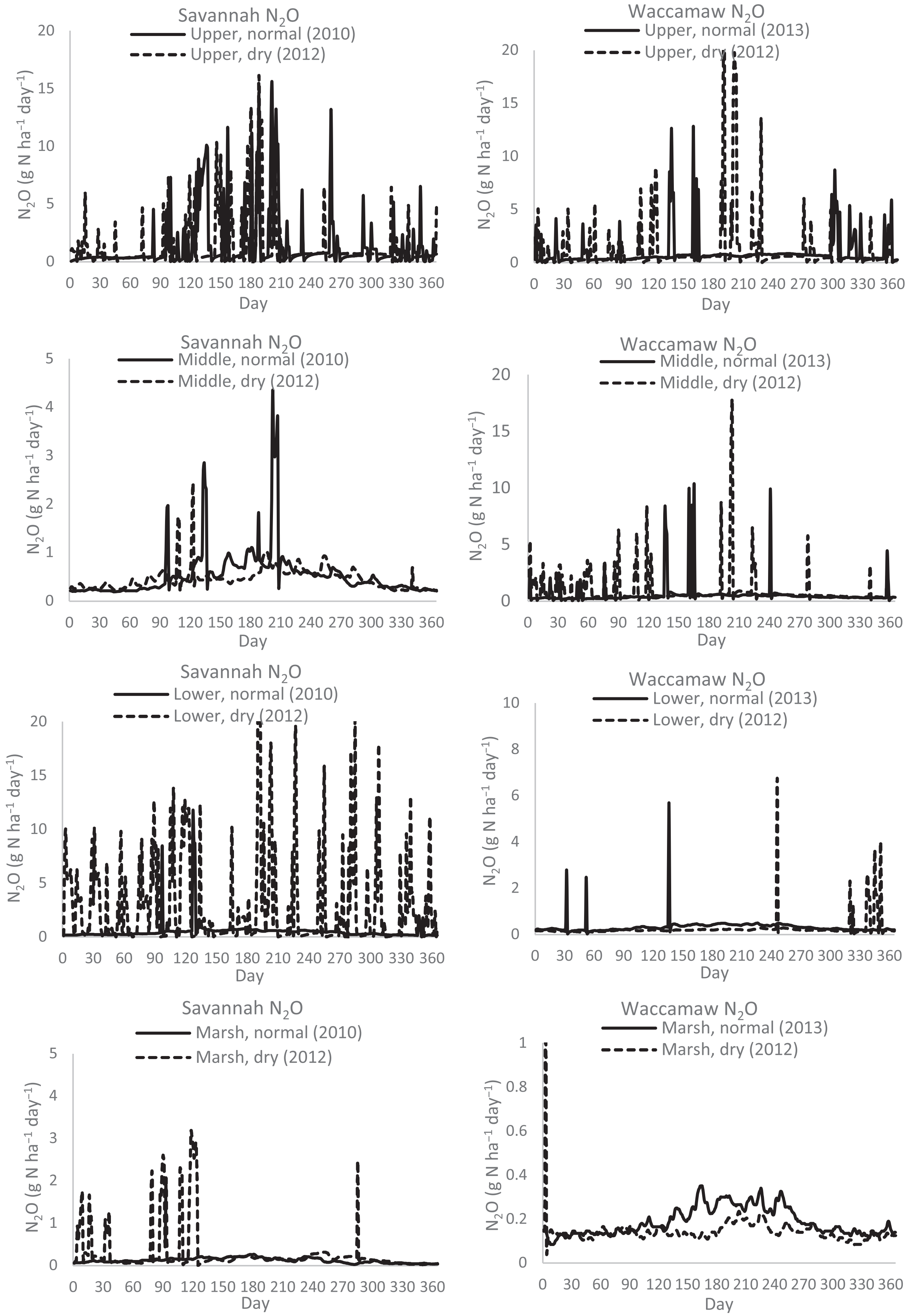

FIGURE 7 Simulated daily soil N_2O emissions under the normal and drought conditions at the upper (top row), middle (second row), lower (third row) forest and oligohaline marsh (fourth row) sites along the Savannah and Waccamaw rivers.

discrete and coarse temporal resolution observations into daily values. Over a restricted temporal scale (e.g., hourly), CH_4 fluxes could be affected by wind speed and atmospheric pressure conditions (e.g., Zhang et al., 2012). There are large diurnal and seasonal variations in CH_4 and N_2O emissions (e.g., Bansal et al., 2018; Cheng et al., 2018). Thus, discrete sampling protocols (e.g., only one or a few times during a day, and a few times during a year) could produce biased estimates of daily, seasonal, and annual emissions when integrating these field measurements over time (e.g., Gutenberg et al., 2019; Roughan et al., 2018; Wood et al., 2013). These situations require a more frequent sampling protocol to overcome, but a biogeochemistry model with fine temporal resolution (e.g., hourly time step) to capture CH_4 and N_2O flux variations within short time intervals, then integrated into daily, monthly, and annual rates, can simulate CH_4 and N_2O fluxes with relatively high accuracy (e.g., Dai et al., 2018b).

In the present study, TFW-DNDC was run on a daily time step. CH_4 and N_2O fluxes in a short time step such as hourly fluxes within tidal cycles were not simulated due to the limited hourly input data (e.g., hydrology, climate, etc.) and output (e.g., CH_4 and N_2O). Representative daily emission fluxes for CH_4 and N_2O are needed for model improvement. TFW-DNDC can be improved by using continuous measurements for a longer temporal scale (e.g., several days or longer, including seasonal) since the variation patterns of CH_4 and N_2O fluxes over a longer time scale are mainly determined by soil processes (e.g., CH_4 production, consumption, and transportation) with less noise from atmospheric conditions (e.g., Zhang et al., 2012). Additionally, contributions of CH_4 emissions by plant-mediated transport, ebullition, and diffusion are incorporated in TFW-DNDC, but there were no field data from our Waccamaw or Savannah sites to calibrate the allocation of these parameters (e.g., diffusion coefficient) in TFW-DNDC; thus, we rely completely on literature values. Furthermore, field measurements of CH_4 and N_2O fluxes in TFFW sites from other coastal regions can be beneficial for model further improvement. In terms of the importance of model parameters, it was found from a model sensitivity analysis (Wang, Dai, Trettin, et al., 2022) that porosity, pH, field capacity, and salt effect factor are critical parameters for improving model accuracy on GHG emission simulations. Previous DNDC studies also found that field capacity is one of the critical model parameters affecting DNDC performance (Gaillard et al., 2018). DNDC tends to underestimate the timing and magnitude of peak N_2O fluxes (Gaillard et al., 2018). TFW-DNDC was also found to underestimate peak N_2O fluxes (Figure 4). This could be attributed to the underestimation of high soil moisture using field capacity and hydraulic conductivity without field measurements. Underestimation of high soil moisture would result in a low rate of denitrification and a high rate of nitrification, leading to low N_2O flux. In DNDC, maximum potential denitrification is a function of soil respiration and soil nitrate concentration (Gaillard et al., 2018). It was found that TFW-DNDC tended to underestimate soil respiration (Wang, Dai, Trettin, et al., 2022). Therefore, more field studies on CH_4 and N_2O fluxes under different soil salinity regimes and soil hydrologic features, such as field capacity and hydraulic conductivity, can help to develop a more representative relationship between salinity and gas fluxes and to incorporate them into the model.

CH_4 emissions

Simulation results showed that under the drought condition, CH_4 emissions would be significantly reduced at all tidal freshwater wetland sites along the Savannah and Waccamaw rivers except the Savannah upper forest site. Across the soil salinity gradient (0–9 psu) for both normal and drought conditions, simulated CH_4 emissions decreases significantly ($p < 0.0001$) with increasing soil salinity (Appendix S1: Figure S1). This study confirmed the observations that CH_4 emissions declined along an increasing soil salinity gradient (e.g., Poffenbarger et al., 2011). Limited laboratory studies also showed that CH_4 production from tidal freshwater forests tends to decline with salinity treatments (0, 2, 5 psu) (e.g., Marton et al., 2012; Minick, Kelley, et al., 2019). For example, Minick, Mitra, et al. (2019) found that methane production was reduced by 98% (wood-free incubations) and by 75%–87% (wood-amended incubations) in saltwater treatments compared to the freshwater plus wood treatments. Reduction of CH_4 emissions at low salinity forest and marsh sites along the two rivers could be attributed to the inhibition of methanogenesis due to the increased activities of sulfate-reducing bacteria with saltwater intrusion. With drought-induced intrusion of saltwater into tidal wetlands, the presence of sulfate in soils would allow sulfate-reducing bacteria to outcompete methanogens for energy sources, resulting in inhibition of methane production by sulfate-reducing bacteria (Holm et al., 2016; Krauss et al., 2016; Poffenbarger et al., 2011).

Reduced CH_4 emissions under drought conditions could also result from increased CH_4 oxidation by methanotrophic bacteria at the soil-atmosphere interface zone and the rhizospheric zone (van der Nat & Middelburg, 2000; Wilson et al., 2015). The direction of CH_4 emission (increase or decrease) is determined by the net outcome between the processes attenuating emission (or stimulation of rhizospheric methane oxidation and suppression of methanogenesis) and those enhancing emission (or transport and simulation methanogenesis) (e.g., van der Nat & Middelburg, 2000). CH_4 oxidation efficiency is generally higher in tidal forests than marshes due to the higher, drier position of forests than marsh on the landscape as well as the development of CH_4-limitation in response to a relatively deep aerobic zone extending 5–10 cm below the surface (Megonigal & Schlesinger, 2002). A significant polynomial relationship ($p = 0.001$) between simulated CH_4 emissions and water level occurred, with large CH_4 emissions tending to occur for soil water level between 5 cm below and 5 cm above soil surface in our study (Appendix S1: Figure S1). When the soil water table declines during drought and changes from saturated to unsaturated conditions, oxidative reactions including methanotrophy, nitrification, and decomposition are enhanced, leading to the increase in soil CO_2 emission and decrease in CH_4 emission (e.g., Cui et al., 2005). Methane production and oxidation are significantly affected by not only salinity and water level, but also soil DOC ($p = 0.02$) and SOC ($p = 0.0008$) (Appendix S1: Figure S1) content. At a local scale, both methanogenesis and methanotrophy may coexist, leading to a net CH_4 emission outcome of increase or no change or decrease. The findings of Krauss and Whitbeck (2012) that salinity (<5 psu) had little consistent effect on CH_4 emissions for Savannah tidal forests and our findings that CH_4 emission tended to decline with soil salinity (0.5–10 psu) under drought-induced saltwater intrusion suggest that the different levels of sulfate concentration in soils and activities of sulfate-reducing bacteria as well as site-specific water level (redox potential) may limit sulfate availability (Bartlett et al., 1987). Methanogenesis may not be inhibited or just partially suppressed for low-salinity (<5 psu) tidal freshwater wetlands. Under the low sulfate concentration, other factors such as soil water level (moisture, or redox potential) and organic carbon availability likely result in the change of the direction of CH_4 emissions from reduction to no change to an increase of CH_4 fluxes. For example, it was found that additions of wood also resulted in higher CH_4 production from saltwater treatments compared to wood-free incubations (Minick, Mitra, et al., 2019). It is also possible that increased salinity could result in increased CH_4 emission due to the reduction in humic substances that decrease CH_4 production by serving as thermodynamically favorable organic electron acceptors, thus leading to the release of methanogens from the inhibitory effects of humics (Ardón et al., 2018).

The increase in CH_4 emission under the drought condition in the Savannah upper forest site indicated that soil water level plays a dominant role in determining CH_4 emission for tidal freshwater wetlands without salinity influence. There was a month-long flooding in February–March in the normal year at the Savannah upper forest site that may explain the low CH_4 emission under the normal condition. It was found that periodic flood pulses can suppress CH_4 emissions, although CH_4 emission increases with water table depth or soil water content in most cases (Altor & Mitsch, 2008). CH_4 emissions could decline due to a diffusion barrier induced by the standing water (Anderson & Lockaby, 2007), potentially resulting in both slow transport and more time for methanotrophy to consume methane. Cui et al. (2005) found that, in tidal forested wetland soils, the uppermost 20 cm is important in controlling CH_4 flux since CH_4 flux could decrease more than 40% when water table drops to >20 cm below the soil surface compared to the 5% decrease in CH_4 flux when water table drops to within 20 cm. Gutenberg et al. (2019) found that much of the variation in CH_4 flux from forested wetland soils of the Great Dismal Swamp in southeastern Virginia is explained by variation in soil moisture from 0 to 5 cm and soil moisture from 5 to 10 cm. Furthermore, available carbon substrate was one of the most important factors affecting CH_4 emission (Morrissey et al., 2014; Vizza et al., 2017). Increased SOC sequestration (substrate available for microbial activity for CH_4 production) in the Savannah upper forest under the drought condition (Wang, Dai, Trettin, et al., 2022) may also be responsible for the increase CH_4 production and emission (as shown in the CH_4-SOC relationship plot in Appendix S1: Figure S1), although CH_4 oxidation could also be elevated (Vizza et al., 2017).

In terms of the seasonal variation in CH_4 emission, the year-round CH_4 emissions in the upper and middle forest sites along the two rivers indicated that CH_4 production and oxidation are mainly controlled by soil water level, or the redox potential status. This is consistent with observations that water table depth is a primary predictor of methane flux rate in a variety of wetlands (Knox et al., 2021). The decrease in daily CH_4 fluxes under the drought condition in the upper and middle forest sites could be attributed to the increased oxidation, suggesting that methanotrophy in upper and middle forest sites tended to be O_2-limited (Megonigal & Schlesinger, 2002). For the lower forest and marsh sites under the normal condition, the increase in CH_4 emission in summer might be related to the stimulated CH_4 production by increased plant growth (van der Nat & Middelburg, 2000). CH_4 emissions in the lower forest and oligohaline marsh sites tended to be completely inhibited by salinity stress under the drought condition when soil salinity increased significantly (larger than 5 up to ~10 psu) (Table 3, Appendix S1: Figure S1). The high simulated redox potential (+258 mV) in the Savannah lower forest site under the drought condition indicated that CH_4 production is completely shut down, but greater CH_4 emissions occurred in late spring, summer, and early fall, rather than early spring and winter under the normal condition with soil salinity <5 psu, suggesting that besides salinity inhibition, CH_4 production is SOM-limited, and oxidation is CH_4-limited (Megonigal & Schlesinger, 2002).

The different responses of CH_4 emissions to drought-induced saltwater intrusion indicate that there appears to be a salinity threshold (non-linear, sensu Chamberlain et al., 2019; Liu et al., 2019) on the change of the direction of CH_4 emission response (Chambers et al., 2011, 2013; Wang et al., 2017; Weston et al., 2006). For tidal freshwater marshes, soil salinity threshold, at which CH_4 emission will significantly decrease, was found to be in the range of 10–15 psu (Chambers et al., 2011, 2013; Poffenbarger et al., 2011; Wang et al., 2017; Weston et al., 2006; Windham-Myers et al., 2018). For tidal freshwater forested wetlands where soils are less frequently inundated than tidal freshwater marshes, and under increasing risk of coastal droughts, a lower salinity threshold such as in the range of 2–5 psu is expected. This is because CH_4 fluxes vary dramatically, and emissions can even increase considerably when sulfate availability is lower (Windham-Myers et al., 2018). Moreover, such a threshold could vary with vegetation type, soil texture, soil temperature, and soil water level (Liu et al., 2019; Wang et al., 2017; Weston et al., 2006). For example, CH_4 fluxes in the Great Dismal Swamp in the southeastern Virginia varied among vegetation types from 0.05 g C m^{-2} $year^{-1}$ for the cedar forest type, to 1.29 g C m^{-2} $year^{-1}$ for maple-gum, and 3.81 g C m^{-2} $year^{-1}$ for pocosin (Gutenberg et al., 2019). CH_4 fluxes were found to increase with soil clay fraction and decrease with soil mean particle size and silt fraction (Batson et al., 2015). Liu et al. (2019) found that higher water levels can alter the intensity and sensitivity of CH_4 flux in response to change in temperature and salinity: at high water levels, the effect of temperature on CH_4 flux is more pronounced with higher CH_4 flux; at low water levels, the effect of salinity is more important, resulting in lower CH_4 flux. Our results also suggest that the salinity threshold on CH_4 emission could vary with sites that have different vegetation composition and soil types, and vary with soil water level, but not soil temperature (Appendix S1: Figure S1). Although temperature is a factor affecting methane emission (Holm et al., 2016; Knox et al., 2021), temperature tended not to be a critical factor on methane emissions at the sites under normal and drought conditions similar as rainfall (Appendix S1: Figure S1). This is because air and soil temperature did not differ significantly between normal and drought conditions at these same Savannah and Waccamaw river sites (Stagg et al., 2017). Furthermore, temperature would not only increase methane production but also methane oxidation (van der Nat & Middelburg, 2000). Additionally, rainfall was found not to affect CH_4 emissions in our forest and oligohaline marsh sites (Appendix S1: Figure S1). Salinity thresholds on CH_4 emissions in the context of the interaction between fine-resolution gradients of soil salinity and water table depth for low salinity (<10 psu) sites with different vegetation and soil characteristics warrant further research. Such salinity and water level thresholds can be explored using TFW-DNDC in addition to field and laboratory experiments.

N_2O emissions

Responses of N_2O emission along the Savannah and Waccamaw rivers were found to be different and inconsistent among the sites (Figure 7). Along the Savannah River, simulated annual N_2O fluxes increased significantly in the lower forest site and oligohaline marsh site but decreased significantly in the middle forest site under the drought condition. In contrast, along the Waccamaw River, simulated annual N_2O fluxes increase significantly in the middle forest site but decrease significantly in the lower forest and oligohaline marsh sites under drought. There are very few studies on N_2O emissions and associated nitrification and denitrification in tidal freshwater forests impacted by salinity. Limited tidal freshwater forest N_2O studies reveal conflicting results on the salinity effect on N_2O emissions, nitrification, and denitrification in tidal freshwater forest soils (Krauss & Whitbeck, 2012; Marton et al., 2012). Regression analysis of modeling results indicated that N_2O emissions decreased with soil salinity when salinity <4 psu but increased with soil salinity when salinity >4 psu (Appendix S1: Figure S2). Lowest N_2O emissions occurred at soil salinity around 4 psu (Appendix S1: Figure S2). It was found that among the Altamaha, Satilla, and Ogeechee rivers in southeastern Georgia, USA, N_2O production increased with salinity (0, 2, 5 psu) only in the Satilla River tidal forest soils, not in soils in the Altamaha and Ogeechee rivers (Marton et al., 2012). Krauss and Whitbeck (2012) found no difference in N_2O emissions from tidal forests along the Savannah River with differing monthly soil porewater salinity (<5 psu). Since N_2O production and consumption are mainly determined by nitrification and denitrification under aerobic and anaerobic soil conditions, the direction of N_2O emissions in tidal freshwater forests reflects the different responses of nitrification and denitrification to changing soil hydrological, physical, and chemical conditions. Modeling results from this study showed that soil salinity coupled with soil water level (soil moisture content), redox potential, and substrate availability (organic carbon, NO_3-N, NH_4-N concentrations) largely determined the magnitude and direction of N_2O emissions under drought-induced saltwater intrusion. Predicted N_2O emissions were significantly related to soil water level, salinity, DOC, SOC, and temperature, but not rainfall. Approximately 66% of variations in N_2O emissions could be explained by soil water level (Appendix S1: Figure S2). Moreover, the effect of salinity on N_2O emissions can be site-dependent (Hu et al., 2020), and reflected by its influence on vegetation productivity, SOM decomposition (e.g., carbon substrates DOC, SOC), as well as concentrations of NO_3^- and NO_2^- through changes in soil moisture, temperature, and redox potential (e.g., Marton et al., 2012).

The increase in N_2O emissions in Savannah lower forest and oligohaline marsh and Waccamaw middle forest sites under the drought condition reflected the enhancement role of salinity in N_2O production when salinity >4 psu (Appendix S1: Figure S2). It was found that denitrification and nitrification are sensitive to salinity (Marton et al., 2012; Wang et al., 2018). Salinity can accelerate nitrification and denitrification activities, and thus N_2O production through stimulating enzymatic activity, and inhibition of N_2O reduction by increased soil H_2S concentration (Doroski et al., 2019; Marton et al., 2012; Morrissey et al., 2014; Weston et al., 2006, 2011). For Savannah marsh and Waccamaw middle forest sites, increased N_2O emissions with increasing soil salinity under the drought condition might also be associated with enhanced Fe(II) level from the increasing salinity (Baldwin et al., 2006), which may result in an increasing denitrification capacity because the Fe(II)-driven nitrate reduction is involved in denitrification (or chemodenitrification).

Increased N_2O emissions under the drought condition also reflected the role that soil water level induces on redox potential and on nitrification and denitrification. Large N_2O emissions were found when redox potential was between +200 and +300 mV (Smith et al., 1983). In the Savannah lower forest site, due to the severe drought (more frequent, long duration of soil water level greater than 20 cm below soil surface), soil redox potential increased from −263 mV under the normal condition to +258 mV under the drought condition, and nitrification was dramatically enhanced, leading to the large increase in N_2O production because nitrification can also produce N_2O during the NH_4^+ oxidation (Murray et al., 2015). The large increase in N_2O emission in Savannah marsh sites under the drought condition may also be related to the lower nitrate loading rate at the oligohaline marsh site (18 μmol N m^{-2} day^{-1}) compared to other sites (44–251 μmol N m^{-2} day^{-1}) (Noe et al., 2013). Under the drought condition, SOM decomposition increased significantly (Wang, Dai, Trettin, et al., 2022), leading to increase in available NO_3-N thus an increase in dentification in this N-limited environment (Korol & Noe, 2020). Available NO_3-N is often used over N_2O as a terminal electron acceptor by denitrifying microorganisms in N-limited ecosystems, and complete denitrification to N_2 is less likely (Megonigal & Neubauer, 2009). The increased N_2O emissions with drought-induced salinity increase could also be attributed to stimulated organic carbon decomposition because labile organic carbon is significantly correlated with N_2O emission rates and denitrification is favored to occur with high availability of organic matter (Li et al., 2019). SOM decomposition rates were found to significantly increase during drought at Savannah lower forest (from 116 to 256 g C m^{-2} $year^{-1}$) and marsh (from 31 to 77 g C m^{-2} $year^{-1}$) sites and Waccamaw middle (from 116 to 169 g C m^{-2} $year^{-1}$) forest sites (Wang, Dai, Trettin, et al., 2022). When soils are drained, rapid decomposition of accumulated labile SOC releases DOC, ammonium, and nitrate, stimulating both nitrification and denitrification to increase N_2O emission (Cui et al., 2005). Increased SOM decomposition could result in increased NH_4^+-N availability that can lead to high rates of coupled nitrification–denitrification (Hu et al., 2020).

Salinity can also inhibit nitrification and denitrification, thereby reducing N_2O emission (e.g., Seo et al., 2008). Denitrification and nitrification decrease strongly with increasing salinity via higher sulfide concentrations in favor of dissimilatory nitrate reduction to ammonium (DNRA) over denitrification (Osborne et al., 2015). The decrease in N_2O emissions in Savannah middle forest and Waccamaw lower forest and marsh sites with increasing soil salinity under the drought condition indicates that salinity, coupled with soil water level, may suppress N_2O emissions by inhibiting denitrification, leading to reduced N_2O emission in tidal wetlands. Liu et al. (2017) found that both water level and salinity significantly affected N_2O emissions from tidal forested wetland soils; decreasing with increasing salinity under flooding conditions (reducing nitrification due to lower available O_2) following soil water content closely during wet-dry cycles. Furthermore, it was found that denitrification was affected by labile organic carbon. Lower SOC sequestration rate (from 358 to 322 g C m^{-2} $year^{-1}$) in Savannah middle forest, and lower net primary production (NPP) at Waccamaw lower forest (from 111 to 36 g C m^{-2} $year^{-1}$) and marsh (from 237 to 208 g C m^{-2} $year^{-1}$) sites could explain the decreased N_2O emissions as a result of decreased carbon substrates. Decreased N_2O emissions in Waccamaw lower forest and marsh sites under the drought condition may also be explained by the sensitivity of N_2O emissions to changes in precipitation. At these two sites, precipitation was found to decrease by 3%–6% under the drought condition compared to the normal condition. It was found that N_2O emissions could decrease 78% with 20% lower precipitation rates but increase 134% with 20% higher precipitation (Stange et al., 2000). Nevertheless, precipitation did not significantly affect N_2O emissions in this study, although N_2O emissions tended to increase with increased precipitation (Appendix S1: Figure S2). Nitrification and denitrification in DNDC models including TFW-DNDC depend on the size of the "anaerobic balloon," which is a simple kinetic scheme predicting the aeration status by calculating oxygen or other oxidants content in the soil profile and strongly increases at higher precipitation rates (Li et al., 2000). Doroski et al. (2019) found that decreased denitrification potential with salinity may be driven by multiple mechanisms including direct microbial and enzyme effects, formation of toxic compounds (i.e., sulfide), and mobilization of nutrients. Increased salinity enhances the flux of NH_4^+ to the water column which can then be exported with tides (Ardón et al., 2018). Export of soil NH_4+ effectively decreases the N supply for coupled nitrification–denitrification in coastal wetlands.

Implications for management

Emissions of CO_2, CH_4, and N_2O from coastal wetland soils can counteract sequestered carbon (Rosentreter et al., 2021), thus making regional wetland carbon assessment more sensitive to statistical assumptions and large uncertainty when upscaling from plot level to landscape level. Modeling results indicate that the responses of CH_4 and N_2O emissions in tidal freshwater forests and oligohaline marshes to drought-induced saltwater intrusion differ greatly by river system and specific site, thus confirming the sensitivity of regional wetland carbon assessment to large uncertainty due to the inconsistent sometimes even conflicting responses of these GHG emissions to climate change and rising sea level. Seven of the eight sites along the Savannah and Waccamaw rivers tended to have reduced CH_4 emissions, and four sites had increased N_2O emissions under the drought condition compared to the normal condition. The remainder of the sites had slightly decreased N_2O emissions. The different responses among sites are largely driven by variations in soil salinity and water table depth. At the Savannah moderate-oligohaline forest site (the lower forest site), up to 80% of the radiative balance from GHG emission is from soil CO_2 release when converted to sustained-flux global warming potentials (CH_4-eq: 19% and N_2O-eq: 1%) based on the estimates of carbon dioxide equivalent of the three gases using the protocol for a 20-year timeframe (Neubauer & Megonigal, 2015). CO_2 release at this lower forest site could increase significantly (120%, Wang, Dai, Trettin, et al., 2022). More tidal freshwater forests will likely convert to moderate-oligohaline forests under future climate change and SLR (Wang, Dai, Trettin, et al., 2022); therefore, the loss of carbon sequestration and accumulation in vegetation and soils of TFFW during the conversion process is inevitable. Carbon sequestration potential may return once healthy marsh develops (Krauss et al., 2018; Smith & Kirwan, 2021). This trend of carbon sequestration capacity loss in tidal freshwater wetlands poses a great challenge to ecosystem-based management of tidal freshwater wetlands that attempt to increase carbon sequestration/storage and reduce carbon loss, including GHG emissions. TFFW managers can take actions to control site water level and soil water table depth to a minimum level (e.g., restoring tidal exchange, Negandhi et al., 2019) to avoid large CO_2 emissions due to drought-induced saltwater intrusion and increases in soil salinity to increase or at least maintain carbon storage under future climate change and SLR. Controlling soil water level and soil salinity (e.g., via structures for controlling the flow and distribution of freshwater and tide) also plays a large role in reducing CH_4 and N_2O emissions especially in late spring, summer, and early fall at upper and middle forest sites when greater CH_4 emissions tend to occur. For example, it was found that a natural tidal treatment had significantly higher carbon storage than an impounded, seasonally drained treatment in tidal freshwater marshes along the lower Waccamaw River (Drexler et al., 2013), demonstrating the importance of restoring tides to enhance carbon storage and reduce methane emissions in impounded wetlands (Kroeger et al., 2017). The presence of surface flooding by tidal inundation could decrease the duration of exposure to freshwater (e.g., rainwater) -induced CH_4 emission (Negandhi et al., 2019), while flooding with saline water may reduce CH_4 fluxes (Kroeger et al., 2017) but change the plant community. Given that the inconsistent and sometimes opposite responses of CH_4 and N_2O emissions in tidal freshwater wetlands to coastal droughts and drought-induced saltwater intrusion seem to be normal, the minimum soil water table depth and soil salinity thresholds that determine the switch of tidal freshwater wetlands from net carbon accumulation to net release of carbon will be dependent on specific site geomorphological, vegetation, soil, and hydrological conditions. Long-term monitoring of soil water level and soil salinity at multiple sites across the salinity gradient from downriver to upriver can help to sort site-specific differences along with model improvements.

In addition, elevated salinity enhanced carbon and nitrogen export by stimulating organic matter decomposition and nitrogen transformation processes, thus decreasing the carbon sequestration and nitrogen retention in tidal wetlands. Salinity can also promote dissimilatory nitrate reduction to ammonia (DNRA) or the H_2S produced by sulfate reduction can interfere with nitrogen cycling by decoupling nitrification—denitrification and producing toxic effects on microbial communities (Wang et al., 2018). DNRA is more important in estuarine and marine systems, whereas denitrification increases in importance in freshwater system (Megonigal & Neubauer, 2009). Furthermore, salinity was observed to increase the abundances of the functional gene groups (Morrissey et al., 2014), which were likely the biotic factors mediating the enhanced CH_4 and N_2O emission rates. Additionally, field data on carbon export (DOC, DIC, POC) to adjacent estuaries and modeling using process-driven biogeochemistry models as TFW-DNDC can help to improve our understanding since carbon export is also a critical component of blue carbon accounting (Krauss et al., 2018) and, thus, the balance between carbon accumulation and loss from tidal freshwater wetlands under changing environment.

CONCLUSIONS

A process-driven biogeochemistry model, Tidal Freshwater Wetland DeNitrification-DeComposition (TFW-DNDC), was applied to examine the responses of CH_4 and N_2O emissions to drought-induced saltwater intrusion in tidal freshwater wetlands along the floodplains of two rivers, the Waccamaw River (South Carolina, USA) and the Savannah River (Georgia and South Carolina, USA) that represent landscape gradients of salinity of both surface water and soil porewater influenced by Atlantic Ocean tides. Analyses of simulation results indicated that the responses of CH_4 and N_2O emissions vary with river system and local geomorphologic settings. The responses of CH_4 and N_2O emissions to drought-induced saltwater intrusion differ in magnitude and could be opposite in direction of change (increase or decrease), reflecting the complicated, nonlinear relationships among ecological processes involved in CH_4 and N_2O emissions and environmental drivers in the dynamic and spatially variable tidal influenced wetlands. Such variable responses of CH_4 and N_2O in TFFW to drought-induced saltwater intrusion pose a large challenge (e.g., increased uncertainty) to the assessment of coastal wetland carbon budgets from plot/site measurements upscaled to landscape estimates. Long-term monitoring of soil water level and soil salinity at sites across the salinity gradient from downriver to upriver from more river systems can help to inform carbon credit-oriented management of tidal freshwater wetlands under future climate change and rising sea level. Measurements of CH_4 and N_2O emission from continuous sampling at multiple sites across the decreasing salinity gradient from downriver to upriver can help to further improve coastal wetland biogeochemistry models, including TFW-DNDC, and tidal freshwater wetland carbon budget assessment.

ACKNOWLEDGMENTS

This research was supported by funds from the U.S. Geological Survey (USGS) Climate Research and Development Program, the USGS Ecosystems Mission Area, and the NASA Carbon Monitoring Systems program to the U.S. Department of Agriculture Forest Service. We thank Melinda Martinez and two anonymous reviewers for their constructive review for improving this manuscript. Any use of trade, firm, or product names is for descriptive purposes only and does not imply endorsement by the U.S. Government.

CONFLICT OF INTEREST STATEMENT

The authors declare no conflicts of interest.

DATA AVAILABILITY STATEMENT

Data for this publication are available from the following repositories and sources: Oak Ridge National Laboratory Distributed Active Archive Center (ORNL DAAC) in Thornton et al. (2022) at https://doi.org/10.3334/ORNLDAAC/2129; U.S. Geological Survey (USGS) ScienceBase in Wang et al. (2020b) at https://doi.org/10.5066/P9JVZZ4N and in Wang, Dai, Krauss, et al. (2022) at https://doi.org/10.5066/P9XDTUX7.

ORCID

Ken W. Krauss https://orcid.org/0000-0003-2195-0729
Carl C. Trettin https://orcid.org/0000-0003-0279-7191
Gregory B. Noe https://orcid.org/0000-0002-6661-2646

REFERENCES

Altor, A. E., and W. J. Mitsch. 2008. "Pulsing Hydrology, Methane Emissions and Carbon Dioxide Fluxes in Created Marshes, A 2-Year Ecosystem Study." *Wetlands* 28: 423–38.

Anderson, C. J., and B. G. Lockaby. 2007. "Soils and Biogeochemistry of Tidal Freshwater Forested Wetlands." In *Ecology of Tidal Freshwater Forested Wetlands of the Southeastern United States*, edited by W. H. Conner, T. W. Doyle, and K. W. Krauss, 65–88. Dordrecht: Springer.

Ardón, M., A. M. Helton, and E. S. Bernhardt. 2018. "Salinity Effects on Greenhouse Gas Emissions from Wetland Soils Are Contingent upon Hydrologic Setting: A Microcosm Experiment." *Biogeochemistry* 140: 217–32.

Baldwin, D. S., G. N. Rees, A. M. Mitchell, G. Watson, and J. Williams. 2006. "The Short-term Effects of Salinization on Anaerobic Nutrient Cycling and Microbial Community Structure in Sediment from a Freshwater Wetland." *Wetlands* 26: 455–64.

Bansal, S., B. Tangen, and R. Finocchiaro. 2018. "Diurnal Patterns of Methane Flux from a Seasonal Wetland: Mechanisms and Methodology." *Wetlands* 38: 933–43.

Bartlett, K. B., D. S. Bartlett, R. C. Harriss, and D. I. Sebacher. 1987. “Methane Emissions along a Salt Marsh Salinity Gradient.” *Biogeochemistry* 4: 183–202.

Batson, J., G. B. Noe, C. R. Hupp, K. W. Krauss, N. B. Rybicki, and E. R. Schenk. 2015. “Soil Greenhouse Gas Emissions and Carbon Budgeting in a Short-Hydroperiod Floodplain Wetland.” *Journal of Geophysical Research: Biogeosciences* 120: 77–95.

Bridgham, S. D., H. Cadillo-Quiroz, J. K. Keller, and Q. Zhuang. 2013. “Methane Emissions from Wetlands: Biogeochemical, Microbial, and Modeling Perspectives from Local to Global Scales.” *Global Change Biology* 19: 1325–46.

Bridgham, S. D., J. P. Megonigal, J. K. Keller, N. B. Bliss, and C. Trettin. 2006. “The Carbon Balance of Norther American Wetlands.” *Wetlands* 26: 889–916.

Chamberlain, S. D., K. S. Hemes, E. Eichelmann, D. J. Szutu, J. G. Verfaillie, and D. D. Baldocchi. 2019. “Effect of Drought-Induced Salinization on Wetland Methane Emissions, Gross Ecosystem Productivity, and their Interactions.” *Ecosystems* 23: 675–88.

Chambers, L. G., T. Z. Osborne, and K. R. Reddy. 2013. “Effect of Salinity-Altering Pulsing Events on Soil Organic Carbon Loss along an Intertidal Wetland Gradient: A Laboratory Experiment.” *Biogeochemistry* 115: 363–83.

Chambers, L. G., K. R. Reddy, and T. Z. Oborne. 2011. “Short-Term Response of Carbon Cycling to Salinity Pulses in a Freshwater Wetland.” *Soil Science Society of America Journal* 75: 2000–7.

Cheng, Y., C. Tong, D. Du, L. Tan, H. Li, and Q. Rao. 2018. “Modeling the Diurnal Variations of Methane Emissions from the Cyperus Malaccensis Tidal Marsh in the Minjiang River Estuary.” *Wetlands* 38: 293–305.

Conner, W. H., J. A. Duberstein, J. W. Day, and S. Hutchinson. 2014. “Impacts of Changing Hydrology and Hurricanes on Forest Structure and Growth along a Flooding/Elevation Gradient in a South Louisianan Forested Wetland from 1986 to 2009.” *Wetlands* 34: 803–14.

Conrads, P. A., and L. S. Darby. 2017. *Development of a Coastal Drought Index Using Salinity Data* 753–66. Boston: BAMS, American Meteorological Society.

Cormier, N., K. W. Krauss, and W. H. Conner. 2013. “Periodicity in Stem Growth and Litterfall in Tidal Freshwater Forested Wetlands: Influence of Salinity and Drought on Nitrogen Recycling.” *Estuaries and Coasts* 36: 533–46.

Craft, C. B. 2012. “Tidal Freshwater Forest Accretion Does Not Keep Pace with Sea Level Rise.” *Global Change Biology* 18: 3615–23.

Cui, J., C. Li, G. Sun, and C. Trettin. 2005. “Linkage of MIKE SHE to Wetland-DNDC for Carbon Budgeting and Anaerobic Biogeochemistry Simulation.” *Biogeochemistry* 72: 147–67.

Dai, Z., C. C. Trettin, S. Frolking, and R. A. Birdsey. 2018a. “Mangrove Carbon Assessment Tool: Model Development and Sensitivity Analysis.” *Estuarine, Coastal and Shelf Science* 208: 23–35.

Dai, Z., C. C. Trettin, S. Frolking, and R. A. Birdsey. 2018b. “Mangrove Carbon Assessment Tool: Model Validation and Assessment of Mangroves in Southern USA and Mexico.” *Estuarine, Coastal and Shelf Science* 208: 107–17.

Doroski, A. A., A. M. Helton, and T. M. Vadas. 2019. “Denitrification Potential and Carbon Mineralization in Restored and Unrestored Coastal Wetland Soils across an Urban Landscape.” *Wetlands* 39: 895–906.

Doyle, T. W., W. H. Conner, R. H. Day, K. W. Krauss, and C. M. Swarzenski. 2007. “Wind Damage and Salinity Effects of Hurricanes Katrina and Rita on Coastal Baldcypress Forests of Louisiana.” In *Science and the Storms–The USGS Response to the Hurricanes of 2005*, edited by G. S. Farris, G. J. Smith, M. P. Crane, C. R. Demas, L. L. Robbins, and D. L. Lavoie, 163–8. Reston: U.S. Geological Survey Circular 1306.

Drexler, J. Z., K. W. Krauss, M. C. Sasser, C. C. Fuller, C. M. Swarzenski, A. Powell, K. M. Swanson, and J. Orlando. 2013. “A Long-Term Comparison of Carbon Sequestration Rates in Impounded and Naturally Tidal Freshwater Marshes along the Lower Waccamaw River, South Carolina.” *Wetlands* 33: 965–74.

Duberstein, J. A., and W. H. Conner. 2009. “Use of Hummocks and Hollows by Trees in Tidal Freshwater Forested Wetlands along the Savannah River.” *Forest Ecology and Management* 258: 1613–8.

Duberstein, J. A., and W. M. Kitchens. 2007. “Community Composition of Select Areas of Tidal Freshwater Forest along the Savannah River.” In *Ecology of Tidal Freshwater Forested Wetlands of the Southeastern United States*, edited by W. H. Conner, T. W. Doyle, and K. W. Krauss, 321–48. Dordrecht: Springer.

Ensign, S. H., C. R. Hupp, G. B. Noe, K. W. Krauss, and C. L. Stagg. 2013. “Sediment Accretion in Tidal Freshwater Forests and Oligohaline Marshes of the Waccamaw and Savannah Rivers, USA.” *Estuaries and Coasts* 37: 1107–19.

Freeman, C., M. A. Lock, S. Hughes, B. Reynolds, and J. A. Hudson. 1997. “Nitrous Oxide Emissions and the Use of Wetlands for Water Quality Amelioration.” *Environmental Science and Technology* 31: 2438–40.

Frenzel, P., and J. Rudolph. 1998. “Methane Emission from a Wetland Plant: The Role of CH4 Oxidation in *Eriophorum*.” *Plant and Soil* 202: 27–32.

Gaillard, R. K., C. D. Jones, P. Ingraham, S. Colier, R. C. Izaurralde, W. Jokela, W. Osterholz, W. Salas, P. Vadas, and M. D. Ruark. 2018. “Underestimation of N2O Emissions in a Comparison of the DayCent, DNDC, and EPIC Models.” *Ecological Applications* 28: 694–708.

Gutenberg, L., K. W. Krauss, J. J. Qu, C. Ahn, D. Hogan, Z. Zhu, and C. Xu. 2019. “Carbon Dioxide Emissions and Methane Flux from Forested Wetland Soils of the Great Dismal Swamp, USA.” *Environmental Management* 4: 190–200.

Hanson, R. S., and T. E. Hanson. 1996. “Methanotrophic Bacteria.” *Microbiological Reviews* 6: 439–71.

Helton, A. M., M. Ardón, and E. S. Bernhardt. 2019. “Hydrologic Context Alters Greenhouse Gas Feedbacks of Coastal Wetland Salinization.” *Ecosystems* 22: 1108–25.

Holm, G. O., Jr., B. C. Perez, D. E. McWhorter, K. W. Krauss, D. J. Johnson, R. C. Raynie, and C. J. Killebrew. 2016. “Ecosystem Level Methane Fluxes from Tidal Freshwater and Brackish Marshes of the Mississippi River Delta: Implications for Coastal Wetland Carbon Projects.” *Wetlands* 36: 401–13.

Hu, M., J. Penuelas, J. Sardans, J. Huang, K. Xu, and C. Tong. 2020. “Denitrification Rates in Tidal Marsh Soils: The Roles of Soil Texture, Salinity and Nitrogen Enrichment.” *European Journal of Soil Science* 72: 474–9.

Jones, M. C., C. E. Bernhardt, K. W. Krauss, and G. B. Noe. 2017. "The Impact of Late Holocene Land Use Change, Climate Variability, and Sea Level Rise on Carbon Storage in Tidal Freshwater Wetlands on the Southeastern United States Coastal Plain." *Journal of Geophysical Research: Biogeosciences* 122: 3126–41.

Kelley, C. A., S. C. Martens, and W. Ussler, III. 1995. "Methane Dynamics across a Tidally Flooded Riverbank Margin." *Limnology and Oceanography* 40(1): 112–1129.

Knox, S. H., S. Bansal, G. McNicol, K. Schafer, C. Sturtevant, M. Ueyama, A. C. Valach, et al. 2021. "Identifying Dominant Environmental Predictors of Freshwater Wetland Methane Fluxes across Diurnal to Seasonal Time Scales." *Global Change Biology* 27: 3582–604.

Korol, A. R., and G. B. Noe. 2020. "Patterns of Denitrification Potential in Tidal Freshwater Forested Wetlands." *Estuaries and Coasts* 43: 329–46.

Krauss, K. W., J. A. Duberstein, T. W. Doyle, W. H. Conner, R. H. Day, L. W. Inabinette, and J. L. Whitbeck. 2009. "Site Condition, Structure, and Growth of Baldcypress along Tidal/Non-tidal Salinity Gradients." *Wetlands* 29: 505–19.

Krauss, K. W., G. O. Holm, Jr., B. Perez, D. E. McWhorter, N. Cormier, R. F. Moss, R.F, D. J. Johnson, S. C. Neubauer, and R. C. Raynie. 2016. "Component Greenhouse Gas Fluxes and Radiative Balance from Two Deltaic Marshes in Louisiana: Pairing Chamber Techniques and Eddy Covariance." *Journal of Geophysical Research: Biogeosciences* 121: 1503–21.

Krauss, K. W., G. B. Noe, J. A. Duberstein, W. H. Conner, C. L. Stagg, N. Cormier, M. C. Jones, et al. 2018. "The Role of the Upper Tidal Estuary in Wetland Blue Carbon Storage and Flux." *Global Biogeochemical Cycles* 32: 817–39.

Krauss, K. W., and J. L. Whitbeck. 2012. "Soil Greenhouse Gas Fluxes during Wetland Forest Retreat along the Lower Savannah River, Georgia (USA)." *Wetlands* 32: 73–81.

Krauss, K. W., J. L. Whitbeck, and R. J. Howard. 2012. "On the Relative Roles of Hydrology, Salinity, Temperature, and Root Productivity in Controlling Soil Respiration from Coastal Swamps (Freshwater)." *Plant and Soil* 358: 265–74.

Kroeger, K. D., S. Crooks, S. Moseman-Valtierra, and J. Tang. 2017. "Restoring Tides to Reduce Methane Emissions in Impounded Wetlands: A New and Potent Blue Carbon Climate Change Intervention." *Scientific Reports* 7: 11914.

Li, C., J. Aber, F. Stange, K. Butgtger-Bahl, and H. Papen. 2000. "A Process-Oriented Model of N2O and NO Emissions from Forest Soils. I. Model Development." *Journal of Geophysical Research Atmospheres* 105: 4369–84.

Li, C., A. Mosier, R. Wassmann, Z. Cai, X. Zheng, Y. Huang, H. Tsuruta, J. Boonjawat, and R. Lantin. 2004. "Modeling Greenhouse Gas Emissions from Rice-Based Production Systems: Sensitivity and Upscaling." *Global Biogeochemical Cycles* 18: GB1043.

Li, X., D. Gao, L. Hou, and M. Liu. 2019. "Salinity Stress Changed the Biogeochemical Controls on CH4 and N2O Emissions of Estuarine and Intertidal Sediments." *Science of the Total Environment* 652: 593–601.

Liu, L., D. Wang, S. Chen, Z. Yu, Y. Xu, Y. Li, Z. Ge, and Z. Chen. 2019. "Methane Emissions from Estuarine Coastal Wetlands: Implications for Global Change Effect." *Soil Science Society of America Journal* 83: 1368–77.

Liu, X. J., A. Ruecker, B. Song, J. Xing, W. H. Conner, and A. T. Chow. 2017. "Effects of Salinity and Wet-Dry Treatments on C and N Dynamics in Coastal-Forested Wetland." *Soil Biology and Biochemistry* 112: 56–67.

Luo, M., J. Huang, W. Zhu, and C. Tong. 2019. "Impacts of Increasing Salinity and Inundation on Rates and Pathways of Organic Carbon Mineralization in Tidal Wetlands: A Review." *Hydrobiologia* 827: 31–49.

Marton, J. M., E. R. Hervert, and C. B. Craft. 2012. "Effects of Salinity on Denitrification and Greenhouse Gas Production from Laboratory-Incubated Tidal Forest Soils." *Wetlands* 32: 347–57.

Megonigal, J. P., and S. C. Neubauer. 2009. "Biogeochemistry of Tidal Freshwater Wetlands." In *Coastal Wetlands: An Integrated Ecosystem Approach*, edited by G. Perillo, E. Wolanski, D. Cahoon, and M. Brinson, 535–62. Boston: Elsevier.

Megonigal, J. P., and W. H. Schlesinger. 2002. "Methane-Limited Methanotroph in Tidal Freshwater Swamps." *Global Biogeochemical Cycles* 16: 1088.

Minick, K. J., A. M. Kelley, G. Miao, X. Li, A. Noormets, B. Mitra, and J. S. King. 2019. "Microtopography Alters Hydrology, Phenol Oxidase Activity and Nutrient Availability in Organic Soils of a Coastal Freshwater Forested Wetland." *Wetlands* 39: 263–73.

Minick, K. J., B. Mitra, A. Noormets, and J. S. King. 2019. "Saltwater Reduces Potential CO2 and CH4 Production in Peat Soils from a Coastal Freshwater Forested Wetland." *Biogeosciences* 16: 4671–86.

Morrissey, E. M., J. L. Gillespie, J. C. Morina, and R. B. Franklin. 2014. "Salinity Affects Microbial Activity and Soil Organic Matter Content in Tidal Wetlands." *Global Change Biology* 20: 1351–62.

Murray, R. H., D. V. Erler, and B. D. Eyre. 2015. "Nitrous Oxide Fluxes in Estuarine Environments: Response to Global Change." *Global Change Biology* 21: 3219–45.

Negandhi, K., G. Edwards, J. J. Kelleway, D. Howard, D. Safari, and N. Saintilan. 2019. "Blue Carbon Potential of Coastal Wetland Restoration Varies with Inundation and Rainfall." *Scientific Reports* 9: 4368.

Neubauer, S. C., R. B. Franklin, and D. J. Berrier. 2013. "Saltwater Intrusion into Tidal Freshwater Marshes Alters the Biogeochemical Processing of Organic Carbon." *Biogeosciences* 10: 8171–83.

Neubauer, S. C., and J. P. Megonigal. 2015. "Moving beyond Global Warming Potentials to Quantify the Climatic Role of Ecosystems." *Ecosystems* 18: 1000–13.

Neubauer, S. C., and J. P. Megonigal. 2022. "Biogeochemistry of Wetland Carbon Preservation and Flux." In *Wetland Carbon and Environmental Management. Geophysical Monograph 267*, edited by K. W. Krauss, Z. Zhu, and C. L. Stagg, 33–71. Hoboken: American Geophysical Union and John Wiley & Sons.

Noe, G. B., N. A. Bourg, K. W. Krauss, J. A. Duberstein, and C. R. Hupp. 2021. "Watershed and Estuarine Controls both Influence Plant Community and Tree Growth Changes in Tidal Freshwater Forested Wetlands along Two U.S. Mid-Atlantic Rivers." *Forests* 12: 1182.

Noe, G. B., C. R. Hupp, C. E. Bernhardt, and K. W. Krauss. 2016. "Contemporary Deposition and Long-Term Accumulation of

Sediment and Nutrients by Tidal Freshwater Forested Wetlands Impacted by Sea Level Rise." *Estuaries and Coasts* 39: 1006–19.

Noe, G. B., K. W. Krauss, B. G. Lockaby, W. H. Conner, and C. R. Hupp. 2013. "The Effect of Increasing Salinity and Forest Mortality on Soil Nitrogen and Phosphorus Mineralization in Tidal Freshwater Forested Wetlands." *Biogeochemistry* 114: 225–44.

Osborne, R. I., M. J. Bernot, and S. E. Findlay. 2015. "Changes in Nitrogen Cycling Processes along a Salinity Gradient in Tidal Wetlands of the Hudson River, New York, USA." *Wetlands* 35: 323–34.

Pierfelice, K. N., B. G. Lockaby, K. W. Krauss, W. H. Conner, G. B. Noe, and M. C. Ricker. 2015. "Salinity Influences on Aboveground and Belowground Net Primary Productivity in Tidal Wetlands." *Journal of Hydrologic Engineering* 22: D5015002.

Poffenbarger, H. J., B. A. Needelman, and J. P. Megonigal. 2011. "Salinity Influence on Methane Emissions from Tidal Marshes." *Wetlands* 31: 831–42.

Reddy, K. R., and R. D. DeLaune. 2008. *Biogeochemistgry of Wetlands: Science and Applications. Chapter 16: Wetlands and Global Climate Change*. Routledge: CRC Press. Taylor & Francis Group.

Rosentreter, J. A., A. N. Al-Haj, R. W. Fulweiler, and P. Williamson. 2021. "Methane and Nitrous Oxide Emissions Complicate Coastal Blue Carbon Assessments." *Global Biogeochemical Cycles* 35: e2020GB006858. https://doi.org/10.1029/2020GB006858.

Roughan, B. L., L. Kellman, E. Smith, and G. L. Chmura. 2018. "Nitrous Oxide Emissions Could Reduce the Blue Carbon Value of Marshes on Eutrophic Estuaries." *Environmental Research Letters* 13: 044034.

Segarra, K. E. A., F. Schubotz, V. Samarkin, M. Y. Yoshinaga, K. U. Hinrichs, and S. B. Joye. 2015. "High Rates of Anaerobic Methane Oxidation in Freshwater Wetlands Reduce Potential Atmospheric Methane Emissions." *Nature Communications* 6: 7477.

Seo, D. C., K. Yu, and R. D. DeLaune. 2008. "Influence of Salinity Level on Sediment Denitrification in a Louisiana Estuary Receiving Diverted Mississippi River Water." *Archives of Agronomy and Soil Science* 54: 249–57.

Smith, A. J., and M. L. Kirwan. 2021. "Sea Level-Driven Marsh Migration Results in Rapid Net Loss of Carbon." *Geophysical Research Letters* 48: e2021GL092420. https://doi.org/10.1029/2021GL092420.

Smith, C. L., R. D. DeLaune, and W. H. Patrick, Jr. 1983. "Nitrous Oxide Emission from Gulf Coast Wetlands." *Geochimica et Cosmochimica Acta* 47: 1805–14.

Stagg, C. L., D. R. Schoolmaster, K. W. Krauss, N. Cormier, and W. H. Conner. 2017. "Causal Mechanisms of Soil Organic Matter Decomposition: Deconstructing Salinity and Flooding Impacts in Coastal Wetlands." *Ecology* 98: 2003–18.

Stange, F., K. Butterbach-Bahl, H. Papen, S. Zechmeister-Boltenstern, C. Li, and J. Aber. 2000. "A Process-Oriented Model of N2O and NO Emissions from Forest Soils 2. Sensitivity Analysis and Validation." *Journal of Geophysical Research* 105: 4385–98.

Theisen, A. R., and J. C. Murrell. 2005. "Facultative Methanotrophs Revisited." *Journal of Bacteriology* 7: 4303–5.

Thomas, B. L., T. W. Doyle, and K. W. Krauss. 2015. "Annual Growth Patterns of Baldcypress (*Taxodium Distichum*) along Salinity Gradients." *Wetlands* 35: 831–939.

Thornton, M. M., R. Shrestha, Y. Wei, P. E. Thornton, S.-C. Kao, and B. E. Wilson. 2022. "Daymet: Daily Surface Weather Data on a 1-km Grid for North America, Version 4 R1." ORNL DAAC, Oak Ridge, Tennessee, USA. https://doi.org/10.3334/ORNLDAAC/2129.

van der Nat, F., and J. J. Middelburg. 2000. "Methane Emission from Tidal Freshwater Marshes." *Biogeochemistry* 49: 103–21.

Vizza, C., W. E. West, S. E. Jones, J. A. Hart, and G. A. Lamberti. 2017. "Regulators of Coastal Wetland Methane Production and Responses to Simulated Global Change." *Biogeosciences* 14: 431–46.

Walter, B. P., and M. Heimann. 2000. "A Process-Based, Climate-Sensitive Model to Derive Methane Emissions from Natural Wetlands: Application to Five Wetland Sites, Sensitivity to Model Parameters, and Climate." *Global Biogeochemical Cycles* 14: 745–65.

Wang, C., C. Tong, L. G. Chambers, and X. Liu. 2017. "Identifying the Salinity Thresholds that Impact Greenhouse Gas Production in Subtropical Tidal Freshwater Marsh Soils." *Wetlands* 37: 559–71.

Wang, H., Z. Dai, K. W. Krauss, C. C. Trettin, G. B. Noe, A. J. Burton, and E. J. Ward. 2022. *Simulated Methane and Nitrous Oxide Emissions under Drought-Induced Saltwater Intrusion in Tidal Freshwater Forested Wetlands*. Reston: U.S. Geological Survey data release. https://doi.org/10.5066/P9XDTUX7.

Wang, H., Z. Dai, C. C. Trettin, K. W. Krauss, G. B. Noe, A. J. Burton, C. L. Stagg, and E. J. Ward. 2022. "Modeling Impacts of Drought-Induced Salinity Intrusion on Carbon Fluxes and Storage in Tidal Freshwater Wetlands." *Ecological Applications* 32: e2700. https://doi.org/10.1002/eap.2700.

Wang, H., K. W. Krauss, G. Noe, C. L. Stagg, C. M. Swarzenski, J. A. Duberstein, W. H. Conner, and D. L. DeAngelis. 2020b. *Modeling Soil Pore Water Salinity Response to Drought in Tidal Freshwater Forested Wetlands*. Reston: U.S. Geological Survey data release. https://doi.org/10.5066/P9JVZZ4N.

Wang, H., K. W. Krauss, G. B. Noe, C. L. Stagg, C. M. Swarzenski, J. A. Duberstein, W. H. Conner, and D. L. DeAngelis. 2020a. "Modeling Soil Porewater Salinity Response to Drought in Tidal Freshwater Forested Wetlands. Journal of Geophysical Research." *Biogeosciences* 125: e2018JG004996.

Wang, H. T., J. A. Gilbert, Y. G. Zhu, and X. R. Yang. 2018. "Salinity Is a Key Factor Driving the Nitrogen Cycling in the Mangrove Sediment." *Science of the Total Environment* 631: 1342–9.

Weston, N. B., R. E. Dixon, and S. B. Joye. 2006. "Ramifications of Increased Salinity in Tidal Freshwater Sediments: Geochemistry and Microbial Pathways of Organic Matter Mineralization." *Journal of Geophysical Research* 111: G01009.

Weston, N. B., M. A. Vile, S. C. Neubauer, and D. J. Velinsky. 2011. "Accelerated Microbial Organic Matter Mineralization Following Salt-Water Intrusion into Tidal Freshwater Marsh Soils." *Biogeochemistry* 102: 135–51.

Wilson, B. J., B. Mortazavi, and R. P. Kiene. 2015. "Spatial and Temporal Variability in Carbon Dioxide and Methane Exchange at Three Coastal Marshes along a Salinity Gradient in a Northern Gulf of Mexico Estuary." *Biogeochemistry* 123: 329–47.

Windham-Myers, L., W.-J. Cai, S. R. Alin, A. Andersson, J. Crosswell, K. H. Dunton, J. M. Hernandez-Ayon, et al. 2018. "Chapter 15: Tidal Wetlands and Estuaries." In *Second State of the Carbon Cycle Report (SOCCR2): A Sustained Assessment Report*, edited by N. G. Cavallaro, R. Shrestha, M. A. Birdsey, R. G. Mayes, S. C. Najjar, P. R. Reed, and Z. Zhu, 596–648. Washington: U.S. Global Change Research Program.

Wood, J. D., R. J. Gordon, and C. Wagner-Riddle. 2013. "Biases in Discrete CH4 and N2O Sampling Protocols Associated with Temporal Variation of Gas Fluxes from Manure Storage Systems." *Agricultural and Forest Meteorology* 171-172: 295–305.

Yu, K., S. P. Faulkner, and M. J. Baldwin. 2008. "Effect of Hydrological Conditions on Nitrous Oxide, Methane, and Carbon Dioxide Dynamics in a Bottomland Hardwood Forest and its Implication for Soil Carbon Sequestration." *Global Change Biology* 14: 798–812.

Yu, K. W., S. P. Faulkner, and W. H. Patrick. 2006. "Redox Potential Characterization and Soil Greenhouse Gas Concentration across a Hydrological Gradient in a Gulf Coast Forest." *Chemosphere* 62: 905–14.

Zhang, Y., C. Li, C. C. Trettin, H. Li, and G. Sun. 2002. "An Integrated Model of Soil, Hydrology, and Vegetation for Carbon Dynamics in Wetland Ecosystems." *Global Biogeochemical Cycles* 16: 1061.

Zhang, Y., T. Sachs, C. Li, and J. Boike. 2012. "Upscaling Methane Fluxes from Closed Chambers to Eddy Covariance Based on a Permafrost Biogeochemistry Integrated Model." *Global Change Biology* 18: 1428–40.

SUPPORTING INFORMATION

Additional supporting information can be found online in the Supporting Information section at the end of this article.

How to cite this article: Wang, Hongqing, Zhaohua Dai, Ken W. Krauss, Carl C. Trettin, Gregory B. Noe, Andrew J. Burton, and Eric J. Ward. 2023. "Modeling Impacts of Saltwater Intrusion on Methane and Nitrous Oxide Emissions in Tidal Forested Wetlands." *Ecological Applications* e2858. https://doi.org/10.1002/eap.2858